



# Geomorphometric comparison of submarine channel-levee complexes with fluvial river systems: observations from the Indus

R. Prerna<sup>1</sup> · Kotha Mahender<sup>2</sup>

Received: 21 October 2019 / Accepted: 7 April 2020 / Published online: 21 April 2020  
© Springer-Verlag GmbH Germany, part of Springer Nature 2020

## Abstract

An analogy between submarine channels and fluvial rivers has existed for long, especially on the basis of planform and morphometry. Underlying this broad resemblance are the minute disparities that shape and control these systems. In order to observe and quantify the variations between submarine channels and subaerial rivers, we present a first-ever geomorphometric investigation of one single system, where the fluvial river is compared with its offshore counterpart from source-to-sink. With exhaustive data from the submarine fan, parameters like longitudinal profile, width, sinuosity, slope and planform of the Indus Fan channel-levee complex (CLC) are estimated and compared on the basis of the same parameters estimated for the fluvial Indus River. Our new data analyses offers key insights into the variable geomorphometric patterns prevalent from the source of the Indus River until the margins of the submarine Indus Fan. Channel width and sinuosity vary from high-to-low downstream in the submarine system and from low to high in the fluvial basin. Characteristic depositional features of either system are mutually exclusive. Longitudinal profiles of the submarine fan and the river basin do not conform—principally due to the difference in intensity of erosional and depositional processes active in both regions. These differences are primarily attributed to a single-point (canyon-fed) distributary flow and a multi-point (tributary-fed) cumulative flow source system, and density contrasts between river flows and turbidity currents. By quantifying this variation, our attempt is to dissuade the long-standing morphometric analogy between fluvial rivers and submarine channels.

**Keywords** Submarine channels · Fluvial river · Geomorphometric comparison · Indus · Channel-levee complex (CLC)

## Introduction

Rivers are formed when headwaters flowing downstream gradually gain momentum and converge under the influence of gravity. These headwaters mostly generate from meltwater or springs/lakes and enhance their erosive capability by gaining stream velocity. The process results in the genesis of an expansive stream network with one major channel called as the river. When such sediment-saturated rivers drain into the sea, streams of turbidity currents are often initiated. If the right conditions prevail, these currents, usually denser than the

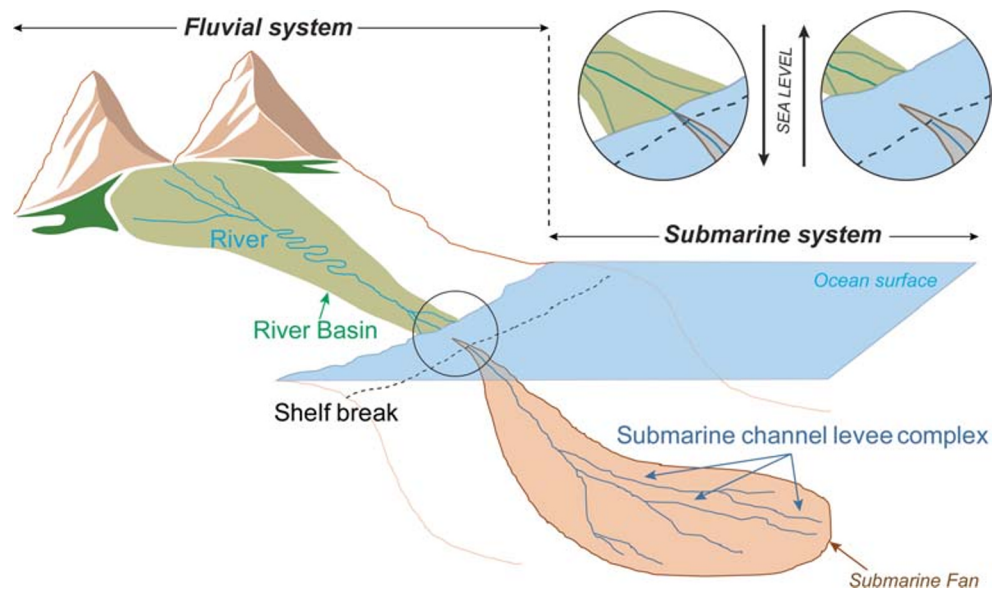
ambient flow, could incise the seafloor and deposit coarser sediments at the bottom while forming fine-grained sediment deposits called levees on the channel flanks. The land-sea terminus, therefore, can be recognized as a juncture where a fluvial river may transform into a submarine channel-levee complex(s) and continue to develop onto the abyssal plains of the ocean floor, up to the point where sediment flux is present and erosion/deposition is active. Factors like sedimentary composition, shelf/slope morphology, tectonic effects and more importantly, eustatic changes are major controls behind submarine channel complex formation (Stow et al. 1985). In the Indus system, specifically, the direct association of sediment supply to canyon head is known to have been largely controlled by eustatic changes (Kolla and Coumes 1987; Shanmugam and Moiola 1988; Prins et al. 2000; Clift et al. 2014). Figure 1 is a simplified schematic representation of the fluvial river basin and the submarine fan system, also depicting direct and indirect association of the canyon head with the fluvial system during low and high sea-stands, respectively.

✉ R. Prerna  
prerna@ncpor.res.in; prerna.geoinfo@gmail.com

<sup>1</sup> National Centre for Polar and Ocean Research, Headland Sada, Vasco-da-Gama, Goa, India

<sup>2</sup> School of Earth, Ocean and Atmospheric Sciences, Goa University, Taleigao Plateau, Goa, India

**Fig. 1** Graphical representation of a typical fluvial and submarine system with associated features depicting direct and indirect association of the canyon head with the fluvial system with sea level change



Much as the rivers on land, submarine channels on the seafloor could be erosive, with the ability to create depositional features and work as conduits for sediment transport. The stark resemblances between fluvial and submarine channels in planform, sinuosity, valley formation etc. lend credence to support the idea of their analogy (Damuth and Flood 1985; Pirmez and Flood 1995; Pickering et al. 1995; Amir et al. 1996; Posamentier 2003; Kolla 2007; McHargue et al. 2011).

On the other hand, there is an equally potent view that finds fluvial channels distinct from submarine channels based on density contrasts of ambient flows, different role of lateral and vertical components of aggradation, migration, rate of meander/levee development, effect of centrifugal/Coriolis forces, relation between slope gradient and sinuosity, base level controls, stratigraphic records etc. (Peakall et al. 2000; Kolla et al. 2001, 2007; Miall 2002; Babonneau et al. 2002; Wynn et al. 2007; Deptuck and Sylvester 2018).

The fluvial-submarine comparison is not a new concept in geomorphic research. Data from offshore submarine fans have been compared with fluvial systems on land, both on a global and regional scale. Clark et al. (1992) summarized data from 16 submarine fan channels and compared them with fluvial/flume data (Leopold and Wolman 1960; Schumm and Khan 1972) to conclude that the geometries of sinuous submarine channels are comparable to fluvial channels as a consequence of analogous physical processes functioning in both systems. Kolla et al. (2001) summarized similarities and differences with respect to channel morphology, evolution, and processes using 3D seismic data from the submarine Congo Fan; however, evidences from fluvial systems were taken from other studies (Flood and Damuth 1987; Clark et al. 1992; Imran et al. 1999; Peakall et al. 2000 etc.). Later, Kolla et al. (2007) presented a comparative paper stressing on the dissimilarities, supported with 3D seismic fluvial channel data from

offshore Indonesia, with submarine channel data from different fans of the world. Konsoer et al. (2013) presented an inventory of 177 submarine channel cross-sections and 216 river cross-sections to substantiate observed differences in channel geometry, evolution, and discharge. Jobe et al. (2016) by comparing 297 submarine and fluvial channel belts from numerous systems across the globe concluded that channel trajectory is the primary control on stratigraphic architecture and that apparently similar channel forms can create clearly different stratigraphy. Several flume-based/laboratory experiments and numerical simulations have also aimed at comparing fluvial and submarine channel behaviour (Imran et al. 1999; Corney et al. 2006; Keevil et al. 2006; Kane et al. 2008; Lajeunesse et al. 2010; Darby and Peakall 2012; Foreman et al. 2015). But what still remains elusive in the quantification of this variation, especially one that is based on data from a singular river-fan system. This approach allows control on the extent of comparison and provides vivid detailing of channel evolution from source-to-sink.

Our study is, therefore, a first-ever geomorphometric comparison with exhaustive data from onshore as well as the offshore basin of the Indus system. Morphometry—a quantitative measure of size and shape—is often used to evaluate the form of any natural feature and geomorphometry is the science of quantitative topographic analysis with focus on the extraction of land-surface parameters from elevation data (Pike 1995; Pike et al. 2009). Its application covers a range of disciplines like earth sciences, environmental engineering, oceanography etc. that aim to capture land-surface parameters like slope, aspect, curvature, stream power and many other morphometric variables from topographic data (Florinsky 2017). In the present study, specific geomorphometric parameters have been analysed to identify and subsequently quantify the variation between submarine channels and fluvial rivers

using Digital Elevation Model (DEM) data and Multibeam Echosounder (MBES) data. Parameters for comparison are longitudinal profile, channel width, sinuosity, channel gradient and planform.

## Study region

The Indus system offers a classic example to study source-to-sink channel morphometry. The Indus Fan and its associated channel levee systems are one of the most complex and expansive submarine fan systems of the world, making it all the more intriguing. On land as well, the Indus River and its basin drain a massive territory of the Indian subcontinent, creating unique morphometric forms as it flows through several tectonic units.

The Indus Canyon is a pre-Holocene relict feature, known to have formed during the low sea levels of the Quaternary when the Indus River extended over the exposed continental shelf coeval with the turbidity currents scouring the shelf (Inam et al. 2008). The extensive erosive flux of the sub-aerial Indus Basin was funnelled offshore via the Indus Canyon into the Arabian Sea—creating the world’s second largest detrital accumulation, i.e. the Indus Fan (Clift et al. 2014) covering an area of approximately 1.1–1.25 million km<sup>2</sup> (Kolla and Coumes 1987; McHargue and Webb 1986). The Indus Fan extends ~1800 km from the Indus Canyon to the Carlsberg Ridge, bound by the Chagos Laccadive Ridge on the east, Owen Fracture Zone to the west and Murray Ridge to the north-west that restrict the fan’s lateral growth (McHargue and Webb 1986). The Upper Indus Fan extends from the foot of the continental slope to the 3400 m isobath; the Middle Indus Fan extends till 3800–4000 m isobaths; and the Lower Indus Fan extends up to the Carlsberg Ridge with depths exceeding 4600 m (Kolla and Coumes 1987). These divisions of the Indus Fan are adopted here to explain channel evolution from the Indus Canyon to the far reaches of the fan.

On land, the transboundary Indus Basin, spreading across Afghanistan, China, India and Pakistan, with an area of 1.16 million km<sup>2</sup> (Winston et al. 2013), forms the twelfth largest drainage basin in the world (Inam et al. 2008). The Chaman Fault and the Karakoram Fault bind the Indus Basin from the W-SW and N-NE, respectively. Prerna et al. (2018) demarcated the Indus Basin into Upper, Middle and Lower basins, based on the physiographic features and morphometric channel behaviour. The Upper Indus Basin extends from the river’s source to the Tarbela Dam shortly after which the river exits the Himalayan Arc. In the Middle Indus Basin, the Kohat Potwar fold belt and the Salt Range are the most significant geotectonic zones, which alter the planform of the Indus River (Kazmi and Jan 1997). After the confluence of the river with its left bank tributaries, the Lower Indus Basin starts—traversed by several basement highs and thrust belts of Kirthar and Sulaiman Ranges (Clift 2017).

Quantitatively, the Indus Basin approximates its submarine fan in terms of area; but does the river follow an analogous morphometric form in both regions is the key research question here. The assumption of similarity between fluvial rivers and submarine channels obscures the fact that similar-appearing planform may not always translate to similarities in internal channel structure, erosion/accretion pattern, flow velocity etc. Figure 2 represents the physiography of the study area and the extent of the different datasets described in “Data and methods”.

## Data and methods

### Data

Two data types are employed in this research—DEM data for fluvial analysis and MBES data for submarine analysis. DEM data used in the study comprises 77 tiles of CartoDEM data (CartoDEM v-3 R1 2015) and 01 tile of SRTM (Shuttle Radar Topography Mission) data (Jarvis et al. 2008) marked as Block F1 and F2, respectively (Fig. 2). MBES data from different parts of the Indus Fan are marked as Block S1, S2 and S3 (Fig. 2). To further constrain our interpretation, inferences from previous works in the Indus Fan—Kenyon et al. (1987) [Block R1]; Kodagali and Jauhari (1999) [Block R2] and Bourget et al. (2013) [Block R3]—are also made. Table 1 enlists the specifications of the multiple datasets used in the study.

## Methods

### Stream/channel extraction

In order to compare the submarine channel and fluvial river behaviour, efficient extraction of the river/channel network from DEM and MBES data was a prerequisite. Since the data for the fluvial Indus River basin was extremely large, manual digitization of the river/streams seemed inept. Hence, a GIS-based model for automated stream network identification and basin delineation was adopted, based on the workflow shown in Fig. 3, executed for every tile systematically as shown in Fig. 4.

Unlike the seamless DEM data for the fluvial basin, MBES data from the submarine fan had certain limitations—(a) data from Blocks S1, S2 and S3 were of variable spatial resolution, and (b) data was fragmented; with voids in certain pockets, and therefore, manual digitization of the channels was more befitting as opposed to automated extraction.

### Parameter estimation

Following the river/channel extraction from both DEM/MBES data was the parametric estimation; parameters being longitudinal profile (built using cross-sections); channel

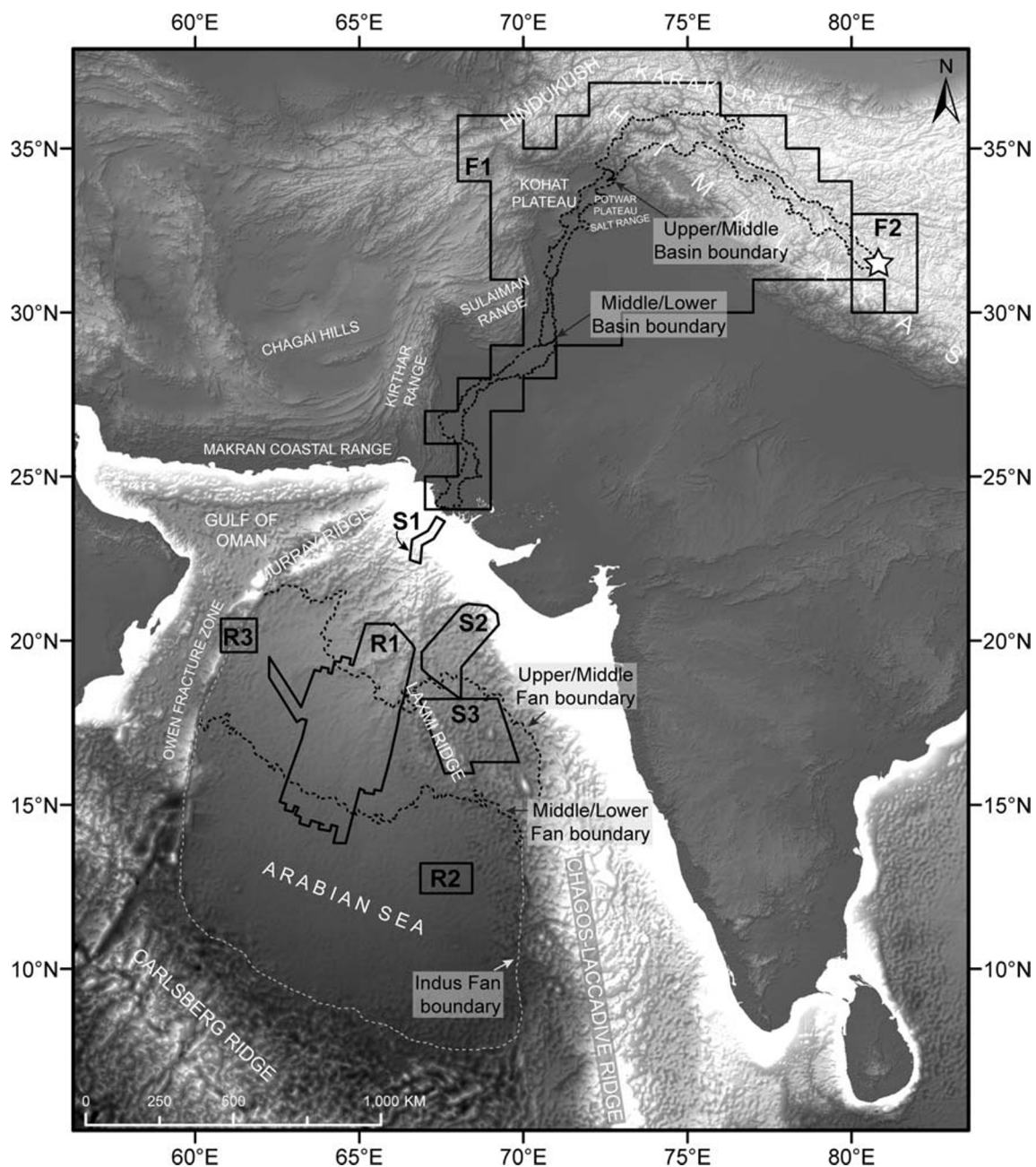


**Fig. 2** Physiographic map of study area. Indus Fan boundaries are adopted from Kolla and Coumes (1987) and Indus Basin boundaries from Prema et al. (2018). Blocks F1 (CartoDEM), F2 (SRTM), S1 (Clift and

Henstock 2015), S2 (NCPOR n.d.), S3 (Mishra et al. 2015), R1 (Kenyon et al. 1987); R2 (Kodagali and Jauhari 1999), R3 (Bourget et al. 2013) represent the extent of datasets. Star represents river source

width, sinuosity, planform and channel gradient, each of which were individually estimated for the Indus fan channels and the Indus River on land. To maintain uniformity in comparison, intervals for parametric estimation were consistent for fluvial and submarine analyses. Channel thalweg was extracted (from cross-sections built every 10 km) to construct the longitudinal profile. In areas where high resolution MBES data was unavailable, seafloor depth from TOPEX mission data (Smith and Sandwell 1997) was utilized. For the channel width profile, straight line transects were drawn perpendicular

to the channel axis, at a 100-m interval for effectively capturing variations in width. Using the cross-sectional area (CSA) approach presented by Qin et al. (2016), channel width is estimated with the lower channel bank as the starting limit, where channel banks occur at different depths. Sinuosity and channel gradient were estimated at 10-km interval. Adopting the conventional method of measuring sinuosity between inflexion points was not possible considering the heterogeneity of the study area and therefore a fixed interval of 10 km was chosen to preserve uniformity in comparison. For

**Table 1** Datasets used for morphometric analysis

Block	DEM data (for fluvial analysis)	Region
F1	CartoDEM (CartoDEM v-3 R1 2015), 30-m ground resolution, $1^\circ \times 1^\circ$ tile	Indus Basin
F2	SRTM (Jarvis et al. 2008), 90-m ground resolution, $5^\circ \times 5^\circ$ tile	
Block	MBES data (for submarine analysis)	Region
S1	Kongsberg EM302 processed bathymetry data, 3.5 kHz frequency, Indus Canyon and shelf, <i>RV Pelagia</i> , Cruise PE300 (Clift and Henstock 2015)	Indus Fan
S2	Processed bathymetry data (NCPOR n.d.)	
S3	SeaBeam 3012 processed bathymetry data, 12 kHz frequency, Laxmi Basin, <i>ORV Sagar Kanya</i> , Cruise SK 306 (Mishra et al. 2015)	
Block	Reference data from previous work	Region
R1	GLORIA long-range sidescan sonar, 3.5 kHz high resolution profiler and precision echo sounder, GLORIA study of the Indus Fan, <i>RRS Charles Darwin</i> , Cruise 20 (Kenyon et al. 1987)	Indus Fan
R2	Hydrosweep processed bathymetry data, 15.5 kHz, Lower Indus Fan, <i>ORV Sagar Kanya</i> , Cruise SK 074 (Kodagali and Jauhari 1999)	
R3	Kongsberg-SIMRAD EM120, 12 kHz, Fanindien 2009 and Owen surveys, <i>RV Beautemps-Beaupré</i> (Bourget et al. 2013)	

representation, the methods for calculating these parameters are shown in Fig. 5 for a single channel in the Middle Indus Fan (1, 2, 3, 4 represent the approach for building longitudinal profile, channel width profile, sinuosity index and channel gradient, respectively).

## Results

### The Indus Fan and the channel-levee complex

The *Indus Canyon* head is evident as a bathymetric incision on the continental shelf. From the base of this Canyon emerge the elaborate CLCs—defined as a series of stacked channel-levee systems fed by the same canyon (Deptuck et al. 2003). Known to have originated as a result of mass wasting and slumping near the river mouth during the low sea level of Pleistocene, the canyon subsequently further developed by retrograde slumping during high sea level (Kolla and Coumes 1987). At present, data from Block S1 shows that the canyon is less than 40 km SSE from the mouth of the river. In the upper reaches of the Indus Canyon, where the canyon incises the shelf, slumping was recorded by Naini and Kolla (1982), which is further corroborated by MBES data (Fig. 6). On the other hand, the lower section is dominated by multiple coherently-spaced terraces (von Rad and Tahir 1997), each separated by near vertical

boundaries (Fig. 6), implicative of erosion and deposition without being disrupted by slumping (Clift et al. 2014). These terraces—defined as topographically flat areas above the channel thalweg but within the channel belt (Hansen et al. 2017), also suggest sequential lateral accretion and vertical erosion, often observed in submarine CLCs (Peakall et al. 2000; Deptuck et al. 2003; Qin et al. 2016). Levee formations are lacking within the canyon, but once the turbidity channels cross the foot of the continental slope, they form large aggradational CLCs with several hundred meters' relief (Kolla and Coumes 1987). Figures 6 and 7 show bathymetric data from the Indus Canyon (Block S1) and Upper Indus Fan (Block S2) with cross-sections representing the transformation in channel morphology. Channel width goes as high as 3 km in the canyon part of the Upper Indus Fan (Fig. 12).

In the *Upper Indus Fan*, data from Block S2 shows channels dissipating into smaller channel-levee systems whilst maintaining lateral aggradation and high sinuosity. Sinuosity Index (SI) is a ratio of curvilinear distance to straight-line distance (Brice 1974). In the Upper Indus Fan, SI values range between 2 and 4 indicating accentuated sinuosity and this continues well into the Middle Indus Fan (Fig. 12). Meandering channels with loops and cut-offs are easily discernible (Figs. 6 and 7). The concept of master bounding levees (Posamentier 2003; Kolla et al. 2007) is adopted here to describe the high relief levee deposits (Fig. 7). At  $\sim 20^\circ\text{N}$



**Fig. 3** Schematic workflow for stream network extraction from DEM

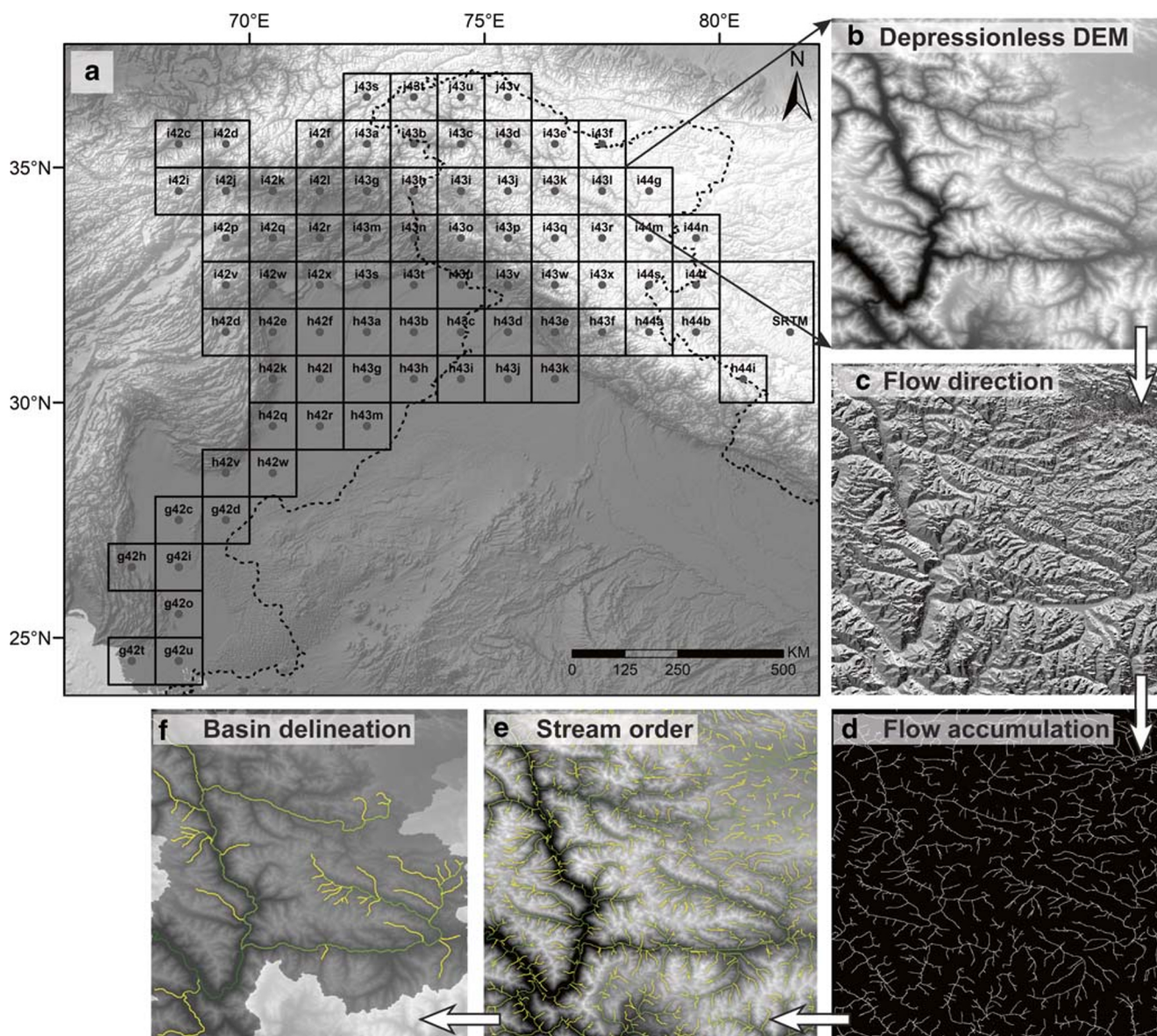


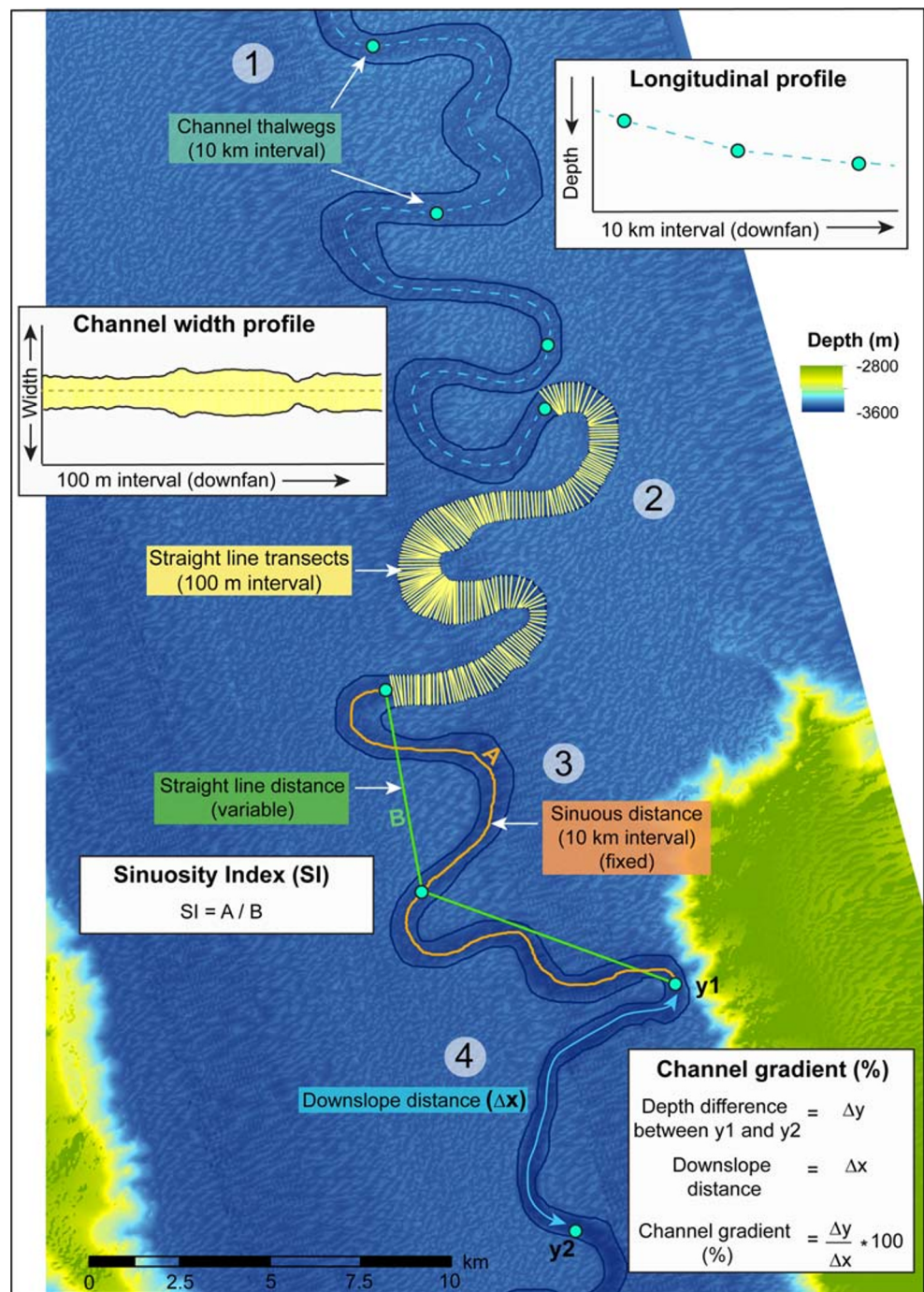
**Fig. 4** **a** Location of 77 CartoDEM and 01 SRTM data tile with grid code used in the study [**b–f** process of stream and basin identification of one tile (i44g) shown as sample]. **b** Depressionless DEM. **c** Flow direction raster. **d** Flow accumulation raster. **e** Stream order. **f** Basin delineation

latitude (3000 m isobath), they start to split as finger-like projections emanating from a larger amalgamated CLC in different directions, spreading tens of kilometres away from one another (Fig. 7). The inner channels are far more sinuous than these master bounding levees, which are products of overflow from several channel loops within their confines. The levees reach maximum height (+ 100 m) in the Upper Indus Fan (P1 to P4, Fig. 7) between 1500 and 3000 m isobaths and develop concomitantly on both flanks of the channel with sediment waves on the outer edges (P3, Fig. 7), similar to those observed by Amir et al. (1996). The cross-sectional views of channels corroborate these findings and help to discern variations as they evolve down-fan. From the confined terrace-

flanked structure in the canyon, they alter morphometrically within the Upper Indus Fan to form elevated master bounding levee type structure.

In the *Middle Indus Fan*, channels attain maximum sinuosity with SI values > 4 at certain locations; however, channel width reduces (Fig. 12). Clark et al. (1992) in their multi-fan study classified Indus Fan as an end-member with high sinuosity developing at relatively lesser gradients (1:400). The Amazon Fan channels also attain highest sinuosity in the middle fan (Flood and Damuth 1987). Average slope gradient as per the data observed is 1:650 in this zone. In some places, channels continue to vertically incise and form considerable levees, with average width of 1 km (Fig. 8).

**Fig. 5** Morphometric parameter estimation from MBES data for a part of the Indus Fan channels. 1 denotes construction of longitudinal profile by plotting thalweg points at 10-km interval; 2 denotes construction of channel width profile using straight line transects at 100-m interval; 3 denotes calculation of Sinuosity Index (SI) using sinuous distance 'A' fixed at 10 km divided by straight line distance 'B'; 4 denotes calculation of channel gradient (as percentage) for every reach of 10 km



Cross-sections constructed along the Middle Indus Fan channels suggest continuity of bifurcated channel-levee systems, as observed in the Upper Indus Fan. The diminishing height of the channel-levees is indicative of reduced turbidity current flow and sediment concentration.

Here, we make a distinction between the relatively low-lying levees observed along the flanks of incisional channel 1 and the bounding levees rising 20–40 m above the seafloor formed by aggradational channels 2 and 3 (Fig. 8). Compared to the other channels, the starkly sinuous planform of the

western-most channel 1 appears to be devoid of bounding levees creating only faint imprints on the seafloor and forming a clear incised valley in the substrate (P1-P2, Fig. 8). The pronounced incision of channel 1 suggests higher erosive capacity, perhaps with greater turbidite flux, but without sediment waves and bounding levees. On the other hand, channels 2 and 3 (P3 to P7, Fig. 8) have bounding levees, albeit, channel 2 plausibly ceases due to its encounter with a geological barrier—the Laxmi Ridge. The levee height of channel 3 is close to 40 m in the north reducing to 20 m downfan above the

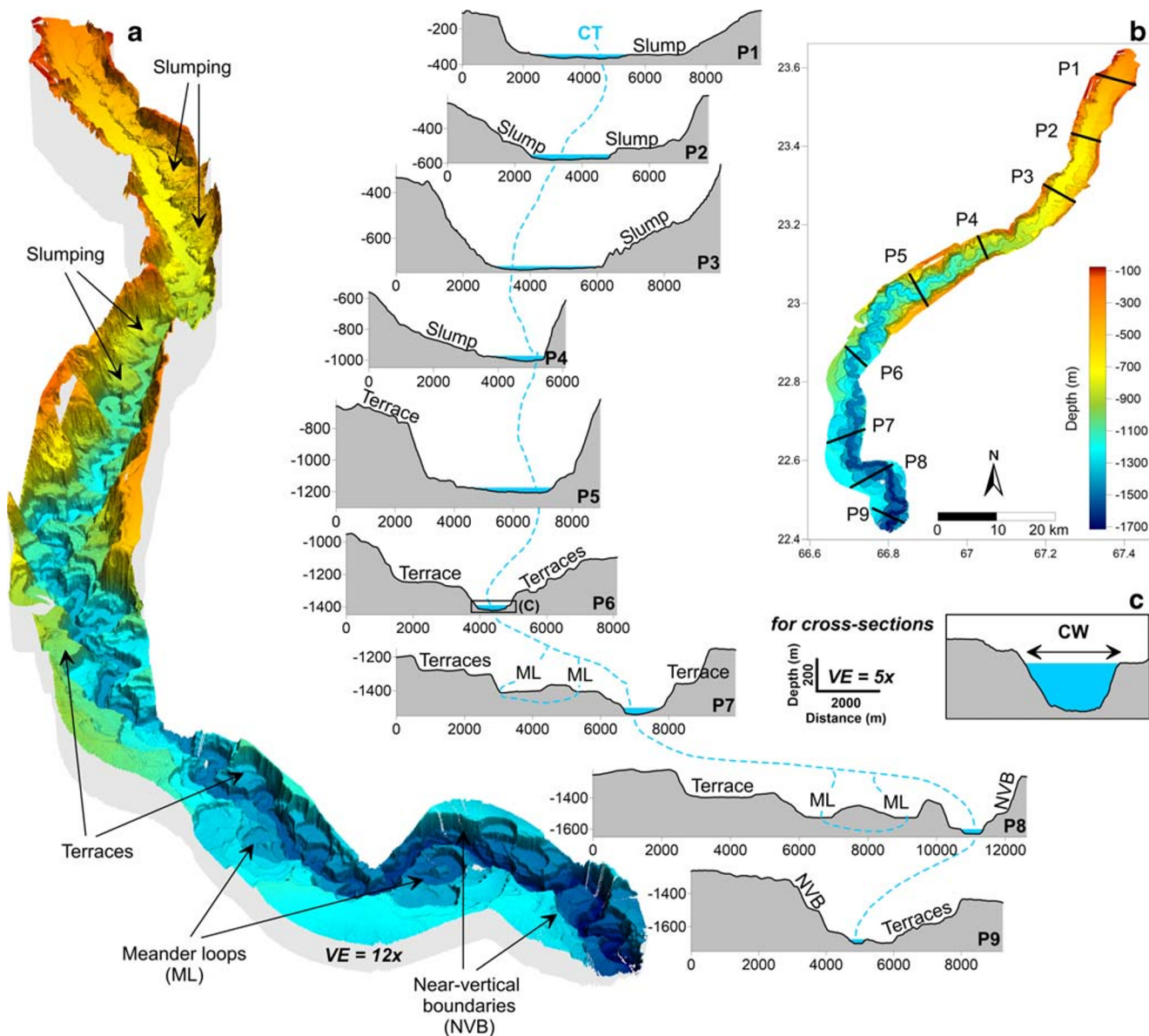


**Fig. 6** **a** 3D surface map of the Indus Canyon (Block S1, refer Fig. 2 for location). Vertical exaggeration (VE) is 12 $\times$ . **b** 2D surface map of the Indus Canyon showing location of cross-sections P1 to P9. Note transition from side wall slumping to flat terraces and near-vertical boundaries

channel thalweg (P5 to P7, Fig. 8). Significant reduction in levee size is seen as a characteristic trait of middle-to-lower fan transition, first observed by Flood and Damuth (1987) in the Middle Amazon Fan. Evidences of sheet-sands or unchanneled turbidity currents in Lower Indus Fan were reported by Kolla and Coumes (1987) and Shanmugam and Moiola (1988). Perhaps, the middle segment of channel 3 is buried by such sheet-sands flowing from the north-east. Within a span of  $\sim 150$  km from west to east, variable channel-levee forms indicate differential erosional/depositional signatures.

A pioneering geophysical survey in the Middle Indus Fan using GLORIA sidescan sonar, seismic profiles and coring

along the channel thalweg. **c** Enlarged representation of box drawn on P6 showing how channel width is estimated [CT: channel thalweg; CW: channel width; ML: meander loop; NVB: near-vertical boundary]

operations reported a distributary complex of large sinuous CLCs forming radial patterns, noted to avulse in the Upper Indus Fan into two distinct bifurcating systems (marked as A and B, Block R1 in Fig. 9) (Kenyon et al. 1987, 1995). System B was suggested to be arising from another proximal canyon (paleo Saraswati Canyon, Fig. 9) linked to the ancient Saraswati River in north-eastern Arabian Sea (Kolla and Coumes 1987; Kenyon et al. 1995). However, on observing the channel paths curving onward into the Middle Indus Fan (Block S2 and S3), the direct association of system B with the Saraswati river and its offshore canyon seems dubious, but the possibility of Saraswati-led channels joining the Indus CLCs cannot be ruled out. With more geophysical data in the future,



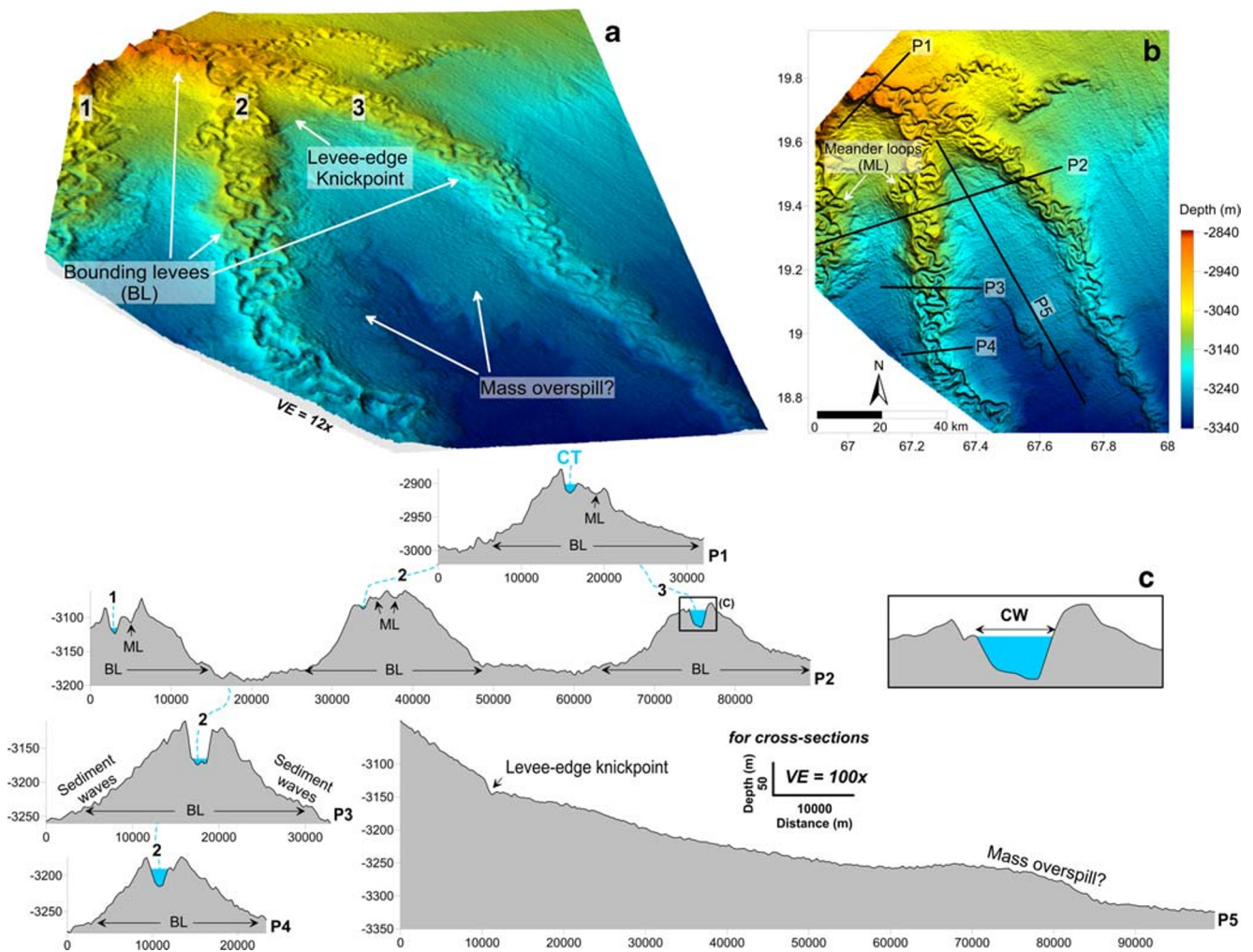


**Fig. 7** a 3D surface map of CLCs in the Upper Indus Fan (Block S2, refer Fig. 2 for location). Vertical exaggeration (VE) is 12×. b 2D surface map of CLCs in the Upper Indus Fan showing location of cross-sections P1 to P5. Note transition in levee height down-fan along the channel thalweg. c

Enlarged representation of box drawn on P2 showing how channel width is estimated [CT: channel thalweg; CW: channel width; BL: bounding levees; ML: meander loop]

both present-day and paleo channel impressions from these auxiliary sources in the Indus Fan could be verified. International Ocean Discovery Program (IODP) drill results from site U1456 (Fig. 9) in the Laxmi Basin have already established the influx of sediments originating from Narmada and/or Tapti River of Western India (Khim et al. 2018). Channels observed in the far west of the Middle Indus Fan from Block R3 (Bourget et al. 2013) seem to have emanated from the ancient Indus canyons and their associated CLCs studied by McHargue and Webb (1986), Kolla and Coumes (1987), Clift et al. (2002) and Berlin (2014). Although their connection must be further corroborated with geophysical observations, their planform does show similarity with those from eastern Middle Indus Fan (Block S3).

In the *Lower Indus Fan*, inferences are limited as it is relatively the least studied section of the Fan. Even so, the continuity of turbidite channels carrying characteristic terrigenous sediments is well established through geophysical

observations and drill operations (Whitmarsh et al. 1974; Naini and Kolla 1982; Kolla and Coumes 1987; Govil and Naidu 2008; Shareef et al. 2018). Another pioneering bathymetric study by Kodagali and Jauhari (1999) (Block R2) affirmed the presence of moderately sinuous channels extending to the Lower Indus Fan with average channel width of 900 m. At a flat surface gradient of 1:1200, channels extend down-fan bound by smaller levees roughly 20 m high with ox-bows (Kodagali and Jauhari 1999). The Mississippi Fan portrays a similar reduction in levee size with reduced sinuosity in its lower fan (Bouma et al. 1985).

**The Indus River and basin**

The Indus Basin—one of the largest fluvial controlled landscapes of the world—showcases unique morphometry due to the sequential effects of the Indus River, and the combined influence of endogenic and exogenic factors, broadly put,

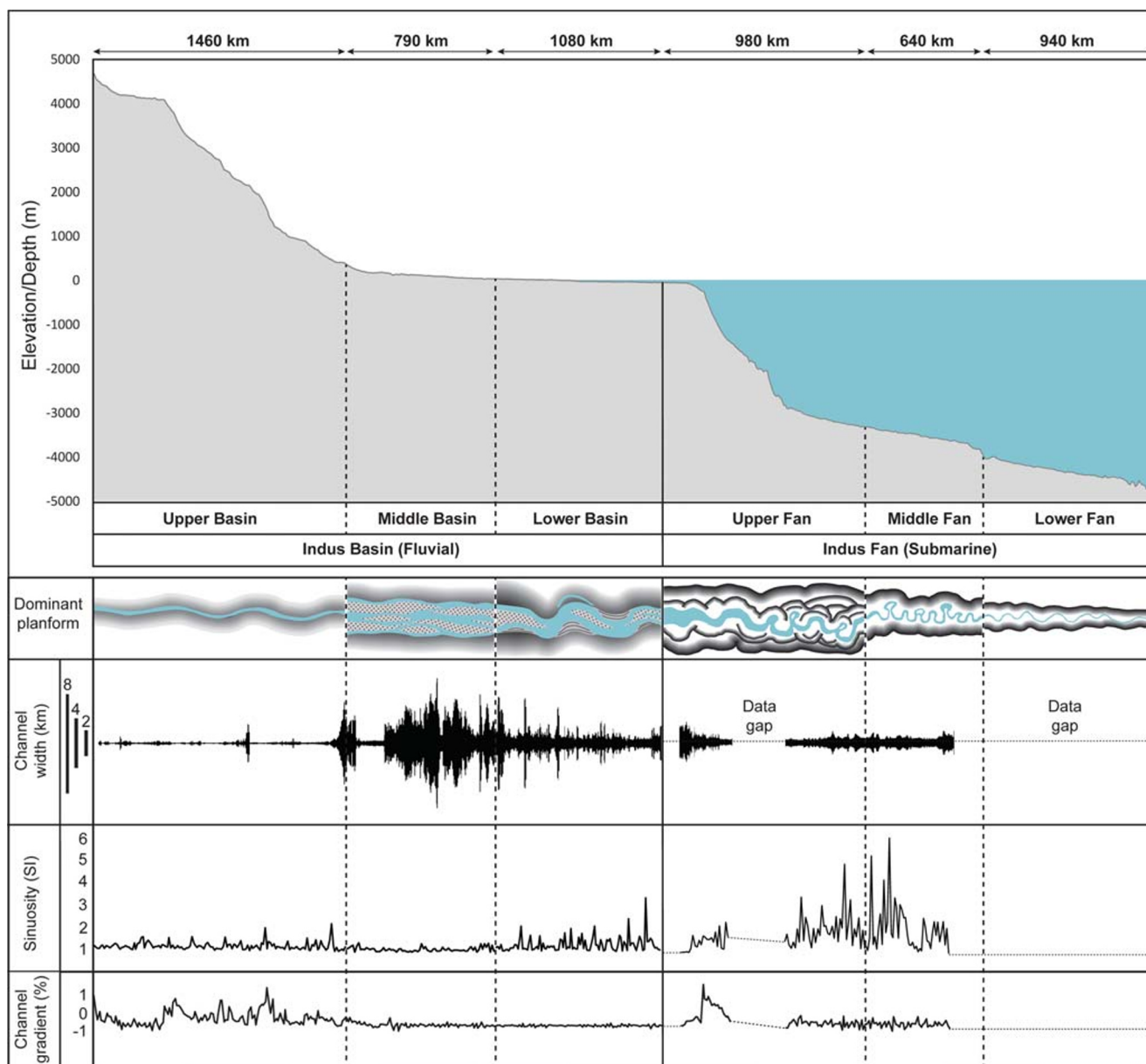


**Fig. 12** Combined longitudinal profile with upper, middle, lower boundaries of the fluvial Indus Basin and the submarine Indus Fan. Dominant planform type, channel width, sinuosity and channel gradient

through each zone of the Indus Basin and Indus Fan denote the transformation of a land-to-deep sea system

tectonic, climatic and anthropogenic influences. The Indus River begins from the confluence of rivers Gar Zangbo and Sênggê Zangbo in the Gangdise Shan Range running on the Tibetan Plateau (Fig. 10). The river sources at 4682 m above sea level and flows for a total length of 3329 km up until its delta (Perna et al. 2018). Despite its large socio-economic relevance in South Asia, a detailed account of its morphometric variations for the entire course remains elusive. Perna et al. (2018) presented a quantitative demarcation of the Upper, Middle and Lower Indus Basin (Fig. 11) based on analyses of critical geomorphometric parameters (viz. longitudinal profiling, channel width, sinuosity, planform, slope

and elevation-relief ratio), and in this study, these demarcations for dividing the Indus Basin are adopted.

The *Upper Indus Basin* represents a zone of rapid incision, downcutting and gorges, resulting from exceptionally high denudation and tectonic uplift (Kazmi and Jan 1997; Ahmed 2013). Lying in the Himalayan complex, this section of the basin is structurally confined, which in effect restricts stream sinuosity. One of the major tectonic influences on river morphometry is attributed to the tectonically active Karakoram Fault (Fig. 10), known to have caused substantive deformation in the region (Searle 1996; Murphy et al. 2000). A significant drop in channel relief is identified where it traverses through

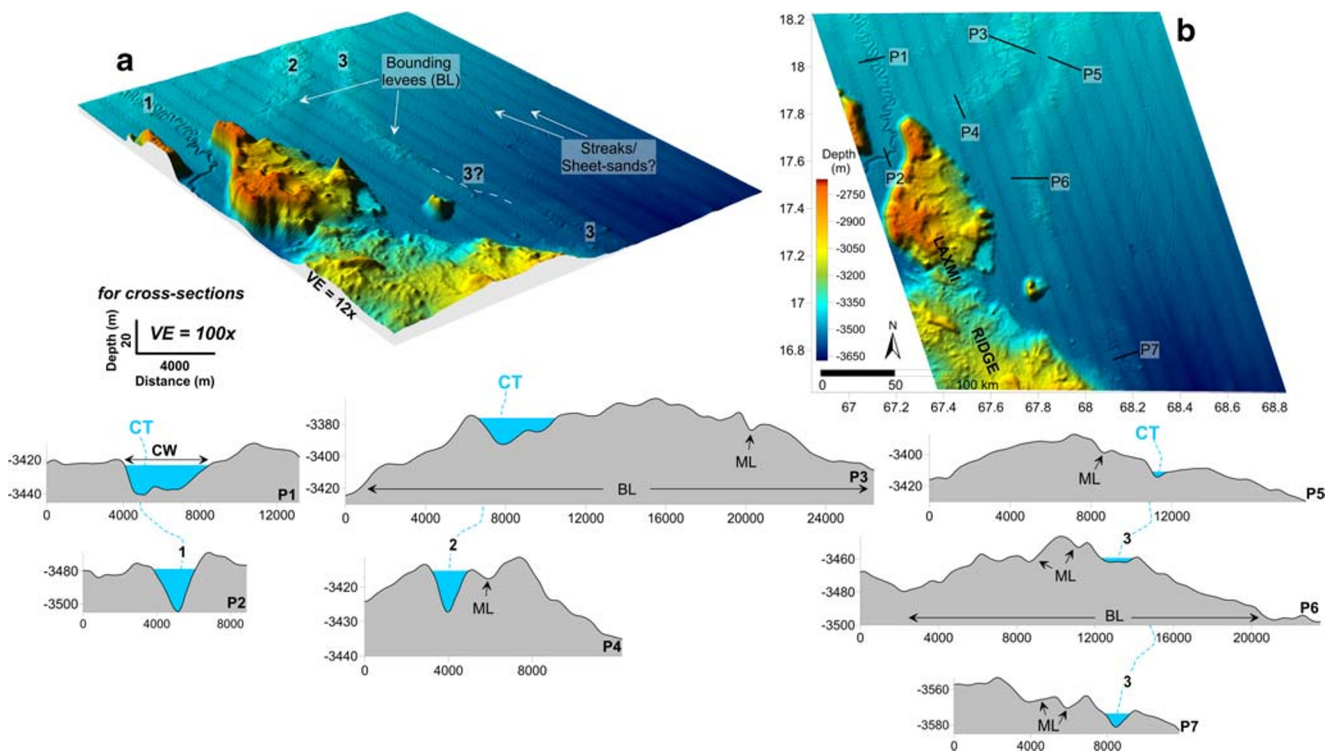


**Fig. 8** **a** 3D surface map of CLCs in the Middle Indus Fan (Block S3, refer Fig. 2 for location) showing three channels numbered 1 to 3. Vertical exaggeration (VE) is 12×. Channel 3 does not show surface impressions in the middle segment denoted by white dashed line. **b** 2D surface map of CLCs in the Middle Indus Fan showing location of cross-sections P1 to

P7. Note distinction between incisional channel 1 without bounding levees and aggradational channels 2 and 3 with bounding levees. The positive relief feature is the Laxmi Ridge [CT: channel thalweg; CW: channel width; BL: bounding levees; ML: meander loop]

the Indus River. Also, at the location of the Tarbela Dam (Figs. 10 and 11), the Upper-Middle Indus Basin boundary (Prerna et al. 2018) is where the river encounters major relief drop as it exits from the Deosai mountain range in Khyber Pakhtunkhwa province of Pakistan and into the flatter plains around Peshawar and Rawalpindi. Until this point, the river is predominantly erosive forming typical v-shaped cross-sections with marginal lateral aggradation, channel width averages at about 250 m and SI values rarely exceed 2 (Fig. 12). Channel gradient is most accentuated in the Upper Indus Basin, given the undulating terrain of the high relief.

In the *Middle Indus Basin*, the river cuts across the Kohat and Potwar Plateau (marked as KP, PP in Fig. 10) before advancing south towards the Salt Range through the Kalabagh gorge. The gorge is known to have caused offset to the course of the Indus (McDougall and Khan 1990; Kazmi and Jan 1997). The river, in this tectonically restricted basin, is characterized by near vertical channel walls with minimal scope for lateral expansion—characterized by narrow channel width, evidently seen on the channel width profile of the Middle Indus Basin (Fig. 12). Once the river opens out into the plains of Sind Sagar Doab, it exhibits distinct depositional lobes and braided stream flow. From thereon, until the confluence of Indus and Panjnad River, which is the Middle-Lower Indus Basin margin (Prerna et al. 2018), the river has a typical

braided form with numerous streams flowing within the channel belt along large elongated sand bars/islands (Fig. 12 and A4, Fig. 13). SI remains < 1.25 because the channel belt is so wide (average 3 km) that appears to have a non-meandering planform (Fig. 12). Average gradient in the fluvial basin is 1:3600.

In the *Lower Indus Basin*, the Indus River undergoes heavy deposition by losing large amount of its transportation capacity at dam/barrage sites (denoted on Fig. 11), widening considerably with evident ox-bows/scroll bars (Prerna et al. 2018) (A5-A6, Fig. 13). During Holocene, the river created a lobate-shaped delta covering most of the Sindh province of Pakistan (Giosan et al. 2006; Inam et al. 2008); however, due to damming and other anthropogenic influences, it stands at a reduced area of 260 km<sup>2</sup> from 2600 km<sup>2</sup> (Kazmi and Jan 1997). Distinct increase in sinuosity, limited braiding, and dominance of a singular channel is the characteristic behaviour observed in the Lower Indus Basin. The basin down to its delta is traversed by a number of basement highs like the Sargodha, Jacobabad etc., (Fig. 10) extending NW-SE for varying distances into uplifted regions (Khan and Clyde 2013). For the last ~300 km of its course (beyond Kotri Barrage, Fig. 11), scroll bars are the only characteristic deposits noticeable along the banks of Indus River, where it flows as a single channel until its delta, with channel width

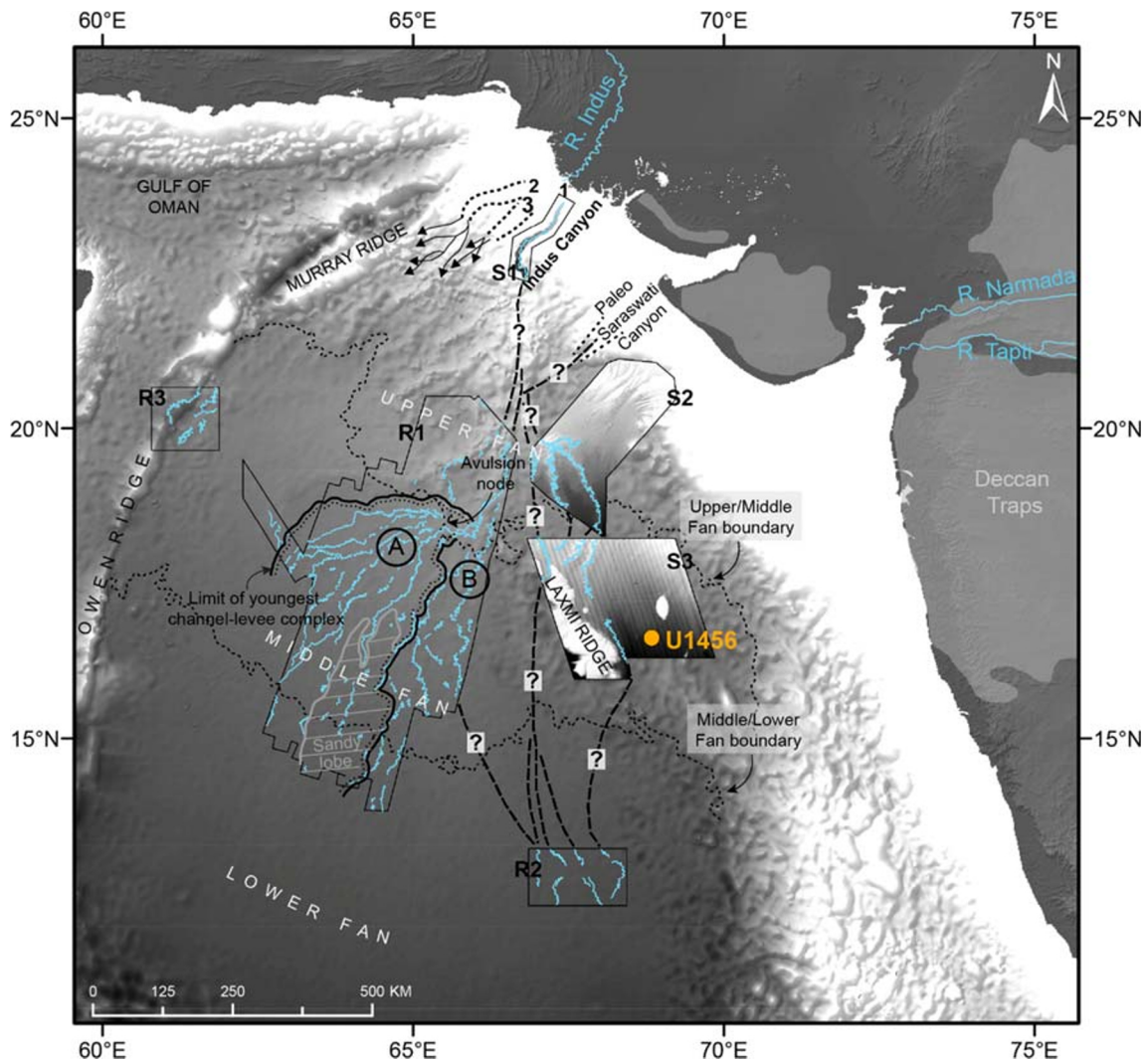


**Fig. 9** Channel network in the Indus Fan with canyon complexes 1–3 (youngest to oldest, modified from McHargue and Webb 1986; Amir et al. 1996). Blue lines represent channels identified from Blocks [S1, S2, S3] and reference Blocks [R1, R2, R3] modified from Kenyon et al.

(1995), Kodagali and Jauhari (1999) and Bourget et al. (2013), respectively. Fan boundaries and paleo Saraswati Canyon adopted from Kolla and Coumes (1987). Black dashed lines indicate probable channel paths; orange circle is the location of IODP Expedition 355 drill site U1456

of 1 to 3 km (Fig. 12 and A6, Fig. 13). Several abandoned channels also extend through this region.

Summarizing the geomorphometric forms observed in the onshore Indus Basin and offshore Indus Fan, Fig. 12 presents the variations in (a) longitudinal profile, (b) channel width, (c) sinuosity, (d) channel gradient and (e) dominant planform type from each zone of both systems.

## Discussion

For a river flowing 3300 km on land and thenceforth as extensive channel levee complexes for at least another 2500 km, the Indus system shows remarkable variability in stream/channel planform from source-to-sink. However, the objective of quantifying this variability between the fluvial and the submarine environment is

met only when geomorphometric parameters are compared. As seen previously, cross-sections are crucial to understand the effects of erosional and depositional processes applying within and along the channel belt. Planforms and cross-sections compared in Fig. 13 imply that the channel form develops from simple-to-complex in the fluvial basin vis-à-vis a complex-to-simple form in the submarine fan. Each zone is characterized by a set of unique channel features, which only result from the variable processes acting upon them.

## Morphometry of the fluvial Indus basin

A smoothly meandering, narrow channel planform with  $SI < 2$  is characteristic of the erosion-dominant high-relief Upper Indus Basin (Fig. 12). The convex-shaped longitudinal profile of this zone of the Indus Basin is useful to identify knick-

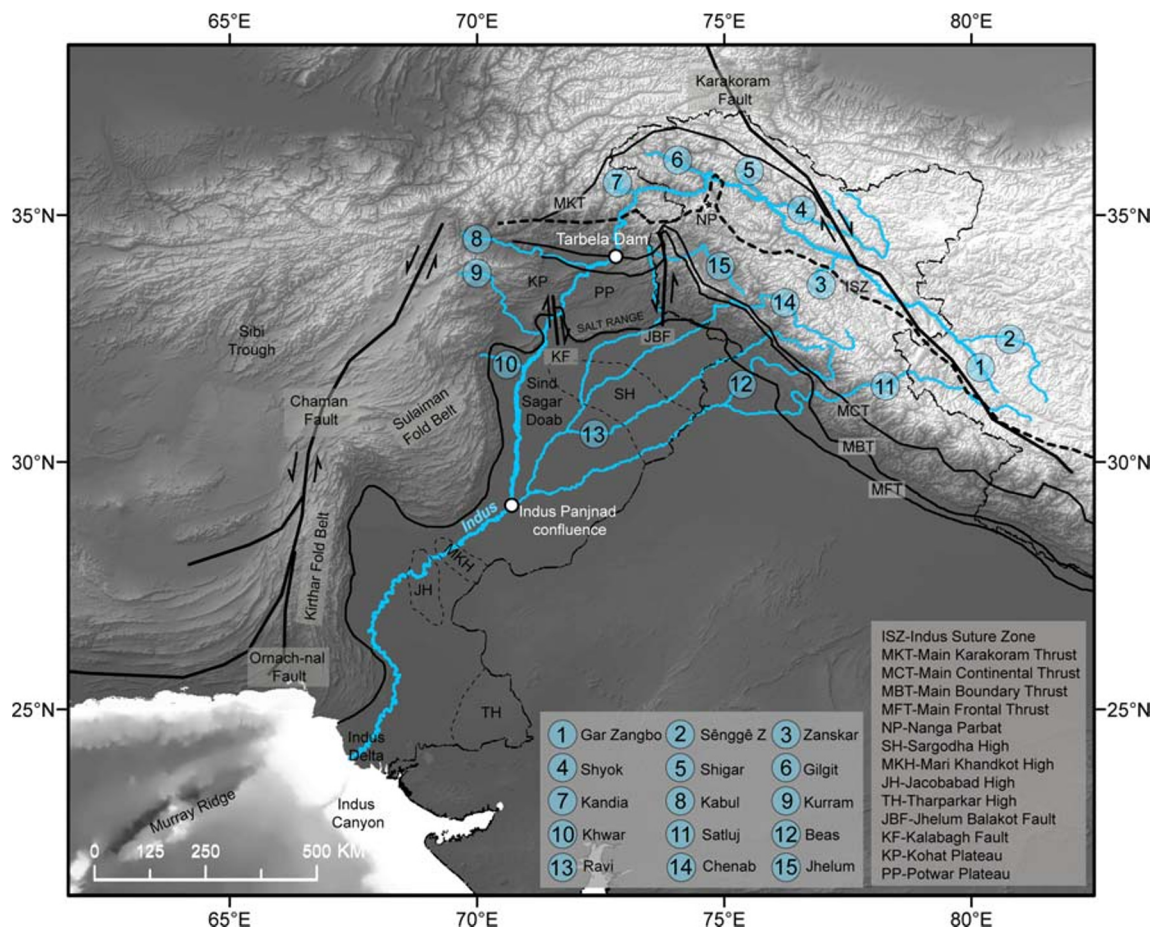


**Fig. 10** Tectonic map of the Indus Basin with major thrust zones/faults marked; modified from Yin (2006), Afzal et al. (2009), Chen and Khan (2010), Asim et al. (2014), Mukherjee (2015) and Prerna et al. (2018). Indus drainage network extracted from CartoDEM data [modified from Prerna et al. 2018]

points where sharp change in gradient is encountered. For most of this region, the river forms a v-shaped valley (A1, Fig. 13) as erosion is stronger than deposition. As a result, channel width is also confined (average 250 m) with infrequent channel widening that represent locations of river confluence in the Upper Indus Basin (Fig. 12). The graph of channel gradient is jagged for most of this zone. Further downstream, the erosive component of river progression gets downplayed by deposition and lateral aggradation is witnessed along cross-sections (A2-A3, Fig. 13).

In the Middle Indus Basin, encountering a drop in relief, channel width rises. In Fig. 12, the transition zone of the Upper-Middle Indus Basin represents this zone of increasing channel width; however, shortly after crossing the Tarbela Dam (location of Upper-Middle Basin boundary), channel width is again restricted as it traverses through the Potwar Plateau. Other than that, the river has an average width of 2700 m in the Middle Indus Basin. Braiding is the dominant planform in this zone with large sand-bars and islands (Fig. 12 and A4, Fig. 13), which is attributable to the construction of dams/barrages along course, and also due to reduced relief causing abrupt deposition. A braided river consists of a single

main channel belt with multiple thalwegs (Makaske 2001), which although may be sinuous by themselves, do not affect the sinuosity of the river. This limits the SI values of the Indus River to < 1.5 (Fig. 12).

In the Lower Indus Basin, average channel width is 1300 m with increasing sinuosity going up to 3 (Fig. 12). Meanders and ox-bows are commonly observed in this zone (A5-A6, Fig. 13). A depositional form with one major channel represents the dominant planform. In all, the channel form grows from a simple-to-complex planform in the fluvial Indus Basin with typical characteristic features of an erosive river with v-shaped valley in the upper basin, braided and depositional form in the middle basin, and finally culminating as a single channel sinuous river with ox-bows and meanders in the lower basin (A6, Fig. 13).

### Morphometry of the submarine Indus Fan

A highly complex channel planform is witnessed inside the Indus Canyon and in the Upper Indus Fan (Fig. 12). In the upper reaches, slumping is dominant (B1, Fig. 13) and further down, flat terraces and near vertical boundaries flank the

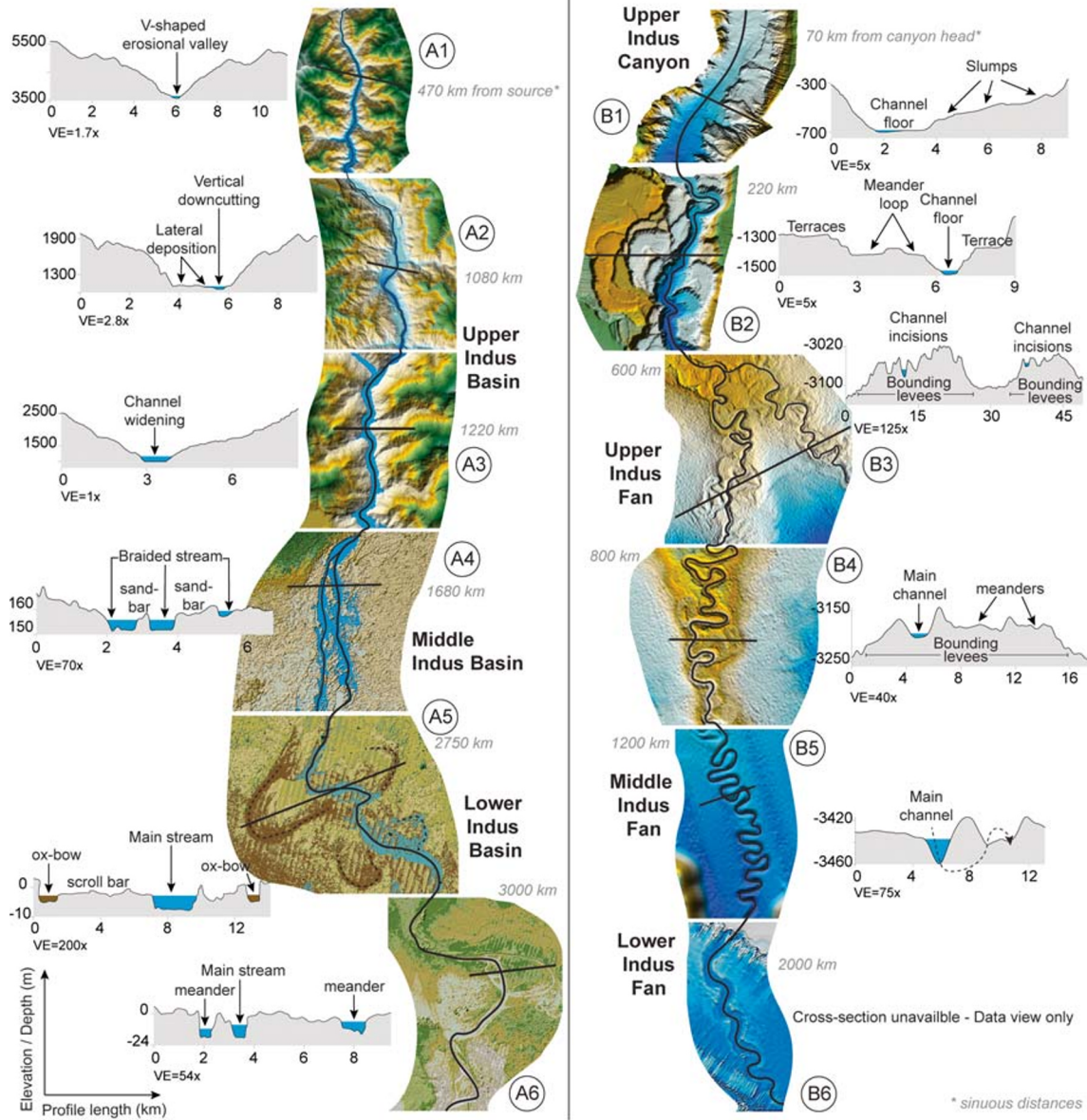


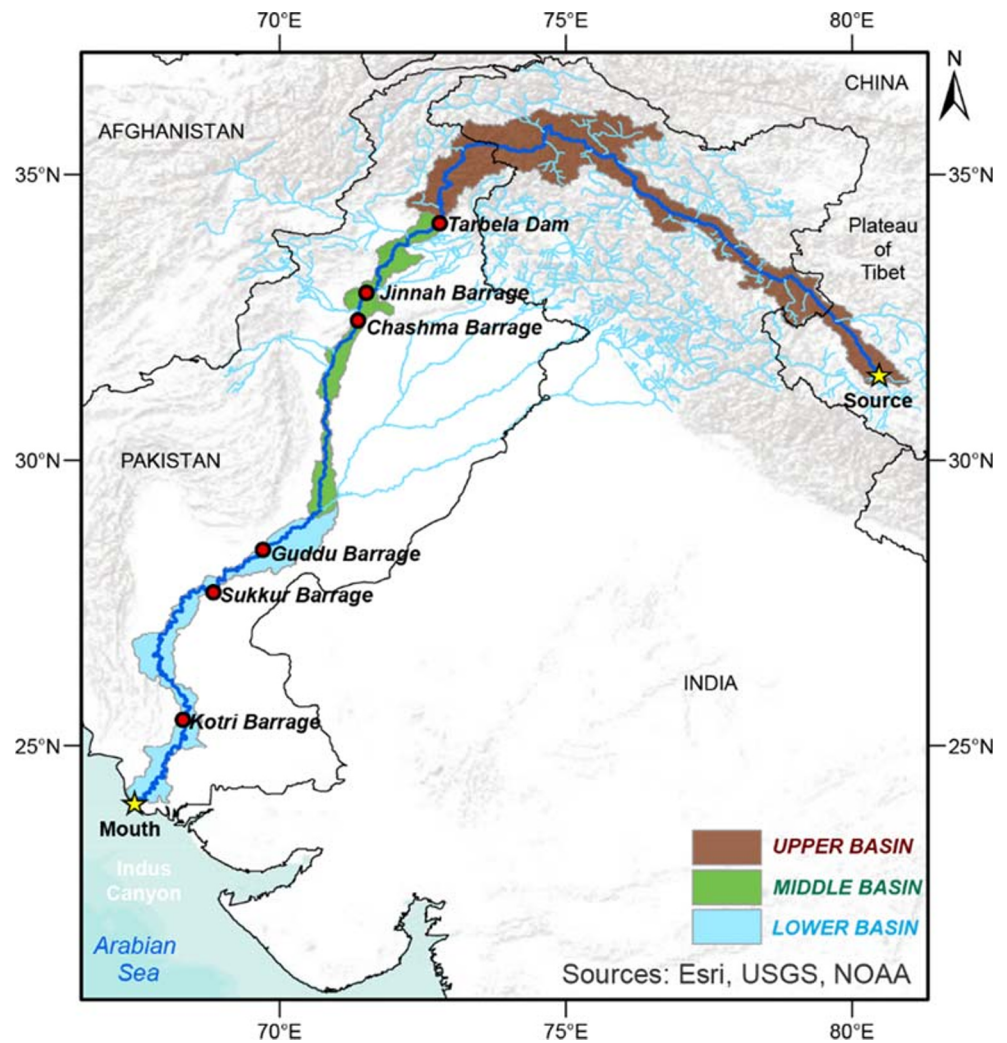
**Fig. 13** Dominant planforms and representative cross-section from the Indus River (A1 to A6) and the Indus Fan channels (B1 to B6). Blue polygons on every cross-section denote channel width [data source: Indus

Basin (Block F1); Upper Indus Canyon (Block S1); Upper Indus Fan (Block S2); Middle Indus Fan (Block S3); Lower Indus Fan (Ward 2007)]

highly sinuous channel belt. Meander loops denote lateral aggradation and vertical downcutting (B2, Fig. 13). The concave-down longitudinal profile of the submarine Indus Fan, especially in the upper reaches, is representative of accentuated erosion that scour the shelfal regions causing sharper gradient change, and channels are at least a km wide throughout the Upper Indus Fan (Fig. 12). Within the Canyon where the channel is already sinuous, on exiting it, channel sinuosity further rises up to 4 in the bifurcating channel-levee systems of the Upper Indus Fan (Fig. 12). As seen previously, high tapering levees (+ 100 m) rising above seafloor are typical in this zone (B3, Fig. 13).

In the Middle Indus Fan, most of these characteristic attributes of channel planform are seen to continue. Meanders are also evident in the bathymetric data from both Upper and Middle Indus Fan. Channel sinuosity is at its maximum in this region; however, further downfan, a reduction is recorded (Fig. 12). Levee heights are reduced and mostly range between 40 and 20 m above the channel thalweg (B4, Fig. 13) and are very faint along incisional channels making only marginal imprints on cross-sections (B5, Fig. 13). The complex dominant planform of the canyon and upper fan gradually evolves into a smoother planform in the Middle Indus Fan (Fig. 12).

**Fig. 11** Indus Basin divided into Upper, Middle and Lower Basin; locations of major dams/barrages are marked along the river (Prerna et al. 2018)



The Lower Indus Basin channel planform is studied from Kodagali and Jauhari (1999) and Ward (2007). As discussed, channels are on average 900 m wide with moderate sinuosity and smaller dimension levees rising around 20 m from the seafloor with evident ox-bows. Therefore, a complex-to-simple planform development is witnessed in the submarine fan. As the distance between the source-point canyon and channel-levee systems increases, channel dimensions reduce and surface deposits become fainter. To summarize:

1. SI values range from 1 to 3.2 in the Indus Basin and from 1 to 5.7 in the Indus Fan (Fig. 12). Maximum channel width on land is observed in the Lower Indus Basin (5–7 km) and in the Upper Indus Fan part of the submarine fan (3–4 km) (Fig. 12). These values suggest that the fairly common trend of increasing sinuosity and channel width from source to mouth in fluvial environments is diametric in the submarine system.
2. Meandering planform, meander loops and ox-bows are symbolic of the mature stage of channel development.

Based on our findings, these are present in the submarine environments right from within the canyon until the Middle Indus Fan (B2 to B4, Fig. 13), and even further till the lower fan (Kodagali and Jauhari 1999). On land, however, they develop mostly in the Lower Indus Basin (A5–A6, Fig. 13). Also, fluvial and submarine planforms in the middle sections of basin/fan are profoundly disparate, ranging from the dominantly braided wide river to the deeply incising sinuous channels.

3. Instead of the broad, smoothly tapering floodplains on land (A4 to A6, Fig. 13), large levees rising > 100 m from the seafloor are seen in the Indus's submarine channel levee complexes, stacked along the flanks of the channels (B3–B4, Fig. 13). Both features result from overspill but their dimensions are contrasting.
4. Terrace formations are observed in both systems, but in variable dimensions and perhaps formed under differing processes/conditions. Evidence of filled and strath terraces on land in the Upper Indus Basin are present (Kumar and Srivastava 2018) but the relatively smaller

**Table 2** Summarized observations on comparison of fluvial and submarine channels

Aspect	Parameters considered	Region	Fluvial basin	Submarine fan
Channel process	Long profile; channel width; SI profile	Upper	Dominantly erosive	Erosive and depositional
		Middle	Dominantly depositional	Erosive and depositional
		Lower	Dominantly depositional	Dominantly depositional
Lateral expansion	Channel width; [ <i>considering width:</i> $\leq 1$ km— <i>low</i> $\geq 1$ km— <i>high</i> ]	Upper	Low (avg. 250 m)	High (avg. 1000 m)
		Middle	High (avg. 2700 m)	High (avg. 1000 m)
		Lower	High (avg. 1300 m)	Low (avg. 900 m)
Sinuosity	SI profile [ <i>considering SI:</i> $\leq 2$ — <i>low</i> $2$ to $3$ — <i>moderate</i> $\geq 3$ — <i>high</i> ]	Upper	Moderate (1 to 2.15)	High (1 to 4.62)
		Middle	Low (1 to 1.39)	High (1 to 5.71)
		Lower	High (1 to 3.22)	Moderate (1 to 2.24)
Meander loops/cut-offs	Planform; cross-sections	Upper	Absent	Present
		Middle	Present	Present
		Lower	Present	Present
Levee height	Cross-sections	Mostly in Middle Basin/Middle Fan	Moderate	Significant
Terrace formation	Cross-sections; planform	Only in Upper Basin/Upper Fan	Present (mostly fluvio-glacially driven; and over-bank spilling)	Evident (driven by sequential lateral and vertical aggradation; and overbank spilling)
Braiding	Planform	Mostly in Middle Basin	Present	Absent

coherently spaced submarine terraces (B2, Fig. 13) probably indicate a higher frequency of vertical erosion and lateral aggradation.

- Braiding is rarely observed in submarine environments (Damuth and Flood 1985; Wynn et al. 2007). Foreman et al. (2015) explained the rarity of braiding in submarine channels due to a combination of factors that induce greater levee deposition and limit channel widening. Nevertheless, lack of evidences of braiding from the Indus Fan suggest that fluvial-like braiding (as seen in A4, Fig. 13) is absent from the submarine system of the Indus. The comparative observations are summarized in Table 2.

## Controlling factors

There is substantial morphometric evidence from the fluvial Indus basin and submarine Indus fan clearly showing nonconformity. Both systems are complex in their own ways with a multitude of factors interplaying. We infer that variance in morphometry is only an indicator of the different processes active in fluvial and submarine systems. A few crucial factors are discussed in this section.

Rivers are almost always joined by tributaries, i.e. multi-point sourced, making the main river a cumulative higher-

order stream with increasing erosive potential as it progresses downstream. Whereas in submarine channel systems, a single conduit (mostly via a canyon head) carrying turbidites gets distributed into several lower order channels with diminishing erosive potential. Deptuck and Sylvester (2018) found submarine and fluvial rivers to be fundamentally different due to the lack of tributaries in a single-point canyon system and because the size of submarine channels reduced down-fan. In the Indus system too, this factor is considered to be the most vital in causing morphometric variation.

Running water and turbidity currents are known to have variable densities, and therefore, they erode and deposit differently. In sediment-gravity currents, flow occurs due to the relatively small difference in unit weight between the gravity fluid and the ambient fluid. The flows of rivers, on the other hand, are seldom considered as gravity currents due to the large difference in unit weight of water and that of air (Middleton 1993). These contrasts cause major differences in the internal architecture and modes of evolution of fluvial and submarine environments (Kolla et al. 2007) and also play a role in controlling depositional products of rivers and channels. Fluvial flood-bank deposits result from overbank flooding; just as submarine levees are created by turbidity currents over-spilling the channel flanks, but the submarine channel levees are typically greater in thickness than in fluvial rivers (Amir et al. 1996). As has been confirmed in our analysis of the



Indus, high relief levees are exclusive to submarine systems only. Wynn et al. (2007) considered these hundred meters plus high aggradational levees as the most spectacular distinction in submarine and fluvial systems.

High sinuosity in submarine channels arises from repeated vertical aggradation and lateral migration instead of only lateral migration as observed in fluvial systems (Kolla et al. 2001). In the Indus Fan too, we believe high sinuosity results from episodic lateral migration and vertical aggradation, although initial seafloor topography would have played a major role. However, in the fluvial Indus Basin, sinuosity is topographically-controlled in the Upper Indus Basin and anthropogenically controlled (by damming) in the Middle and Lower Indus Basin (Perna et al. 2018). Jobe et al. (2016) compared stratigraphic patterns of numerous fluvial and submarine channel systems to conclude that vertical aggradation is stronger in submarine systems with lateral accretion being more dominant in fluvial systems. High incidence of lateral migration is also noted only in the fluvial Indus Basin because valley entrenchment is significantly low compared to the submarine extent where high valley entrenchment (by levees) obstructs channel widening. Hence, the functioning of erosive/depositional elements during channel development could differ significantly in the two systems.

Channel width and channel depth are often studied to assess the erosive and depositional potential of a river system. Flood and Damuth (1987) while comparing the Amazon Fan channels to fluvial rivers concluded that channel width, depth, levee size and cross-sectional area reduced down-fan, which was in contrast to subaerial rivers where the sediment discharge increases downstream with more tributaries adding into the main stream. In our analysis of the Indus Basin and Fan, we find that channel width increases in the fluvial basin and reduces in the submarine fan. Cross-sections from the Upper, Middle and Lower Indus Fans confirm a downward trend of channel depth as well. The major controller for this distinction could be the influence of a single-point and a multi-point source of flow. In single point-source channel-fan systems such as the Indus, Amazon (Flood and Damuth 1987) or Zaire (Babonneau et al. 2002), as the distance from the source point increases, the erosive strength of the channels and the thickness of turbidity currents reduce, thereby making the channels' cross-section smaller, and levees thinner.

## Conclusion

This geomorphometric investigation aims to (a) quantify the variation between fluvial river and submarine channel morphology with comparative data from the Indus's fluvial and

submarine system and (b) to suggest the causative factors behind the differences observed.

The Indus River begins as a narrow, erosive and moderately sinuous stream in the structurally controlled Upper Indus Basin. On encountering drop in relief in the Middle Basin, the river spreads laterally in a braided form, causing excessive channel widening, but with low sinuosity. And in the Lower Indus Basin, the river transforms from a braided (less sinuous) river into a single channel (highly sinuous) river, with several scrollbars and ox-bows as part of its planform, and continues so till it meets the sea.

The Indus Fan channel systems exhibit divergent morphometry. In the Upper Indus Canyon, near-vertical walls and terrace formations indicate inner-levee deposition, vertical aggradation and lateral migration. After exiting the canyon in the Upper Indus Fan, the highly sinuous channel diverges into several radially spreading lower-order channels, which also demonstrate coeval incision and deposition creating high-relief bounding levees—characteristic of the region. In the Middle Indus Fan, they continue to flow creating large bounding levees or low-lying levees with significant channel sinuosity. Reduced valley depth down-fan is indicative of reduced sediment flux and overspill. Narrow channels with low sinuosity, insignificant levees and very shallow thalwegs are characteristic of the Lower Indus Fan.

Parameters used here to capture the geomorphometric behaviour of fluvial rivers and submarine channels were only indicators of the underlying phenomena. Principal causative factors for geomorphometric variation in fluvial rivers and submarine channels are (a) multi-point versus single-point source system i.e. presence and absence of tributaries, respectively; (b) increasing sediment flux in fluvial systems downstream versus distributary-like division in submarine systems; and (c) differences in functioning of erosional/depositional elements during channel development. These, in effect, cause differences in characteristic depositional features and their dimensions, e.g. flat-wide floodplains vs. high-tapering bounding levees, and cause channel dimensions to progressively increase and decrease in fluvial rivers and submarine channels, respectively.

Given that every system is unique in its own form, with variable tectonic and topographic conditions, sediment flux, flow velocity etc., a generalized model can only be built if the system is studied in its entirety. We believe that studies like this could help build a wider picture of the entire canyon-fed channel-levee-lobe system. Other controlling factors like effects of Coriolis and centrifugal forces, base-level attainment, steady flows and catastrophic flows, vertical and horizontal density gradients, helical flow behaviour are believed to have a diametric influence on shaping the morphometry of fluvial and submarine channels (Imran et al. 1999; Kolla et al. 2001, 2007; Corney et al. 2006; Keevil et al. 2006; Peakall and Sumner 2015) and must be explored further in the context of

the Indus system. Wynn et al. (2007) exhaustively studied fan systems across the globe and opined against that the long-held notion of similarities between fluvial river systems and submarine channel systems solely based on observable planform morphology. The research outcome from this study is also purely based on planform and geomorphometry, but corroborated with fluvial and submarine data of a single river system. These evidences are crucial to conclude that submarine channels and fluvial rivers are similar only superficially and must not be considered similar in form and function.

**Acknowledgments** The authors would like to thank Director, NCPOR, Goa for extending continued support to carry out this research. Exclusive Economic Survey Group from NCPOR, Goa is sincerely thanked for providing MBES data from Upper Indus Fan and; Dr. Peter D Clift and Dr. Tim Henstock for permitting the use of MBES data from the Indus Canyon (accessed from Marine Geophysical Data System [www.marine-geo.org](http://www.marine-geo.org)) without which this research could not have been as expansive and well-constrained. Dr. Dhananjai K Pandey and Mr. Ajeet Kumar are also graciously thanked for their kind support. This is NCPOR Contribution No. J-02/2020-21.

## Compliance with ethical standards

**Conflict of interest** The authors declare that they have no conflict of interest.

## References

- Afzal J, Williams M, Aldridge RJ (2009) Revised stratigraphy of the lower Cenozoic succession of the greater Indus Basin in Pakistan. *J Micropalaeontol* 28(1):7–23. <https://doi.org/10.1144/jm.28.1.7>
- Ahmed MF (2013) A regional study of landslide hazards and related features in the upper Indus River Basin, northern Pakistan. Doctoral Dissertations. Paper 2109. [http://scholarsmine.mst.edu/doctoral\\_dissertations/2109](http://scholarsmine.mst.edu/doctoral_dissertations/2109)
- Amir A, Kenyon NH, Cramp A, Kidd RB (1996) Morphology of channel-levee systems on the Indus deep-sea fan, Arabian Sea. *Pakistan J Hydrocarbon Res* 8(1):43–53 <https://pjhrr.org.pk/index.php/pjhr/article/download/97/89/>
- Asim S, Qureshi S, Asif S, Abbasi S, Solangi S, Mirza M (2014) Structural and stratigraphical correlation of seismic profiles between Drigri Anticline and Bahawalpur High in Central Indus Basin of Pakistan. *Int J Geosci* 5(11):1231–1240. <https://doi.org/10.4236/ijg.2014.511102>
- Babonneau N, Savoye B, Cremer M, Klein B (2002) Morphology and architecture of the present canyon and channel system of the Zaire deep-sea fan. *Mar Pet Geol* 19(4):445–467. [https://doi.org/10.1016/S0264-8172\(02\)00009-0](https://doi.org/10.1016/S0264-8172(02)00009-0)
- Berlin TL (2014) Channel-levee complexes and sediment flux of the upper Indus Fan. LSU Master's Theses. 1236. [https://digitalcommons.lsu.edu/gradschool\\_theses/1236](https://digitalcommons.lsu.edu/gradschool_theses/1236)
- Bouma AH, Stelling CE, Coleman JM (1985) Mississippi Fan: Gulf of Mexico. In: Bouma AH, Normark WR, Barnes NE (eds) *Submarine fans and related turbidite systems: frontiers in sedimentary geology*. Springer, New York, pp 143–150. [https://doi.org/10.1007/978-1-4612-5114-9\\_21](https://doi.org/10.1007/978-1-4612-5114-9_21)
- Bourget J, Zaragosi S, Rodriguez M, Fournier M, Garlan T, Chamot-Rooke N (2013) Late Quaternary megaturbidites of the Indus fan: origin and stratigraphic significance. *Mar Geol* 336:10–23. <https://doi.org/10.1016/j.margeo.2012.11.011>
- Brice JC (1974) Evolution of meander loops. In: Kolla V, Bourges P, Urruty J-M, Safa P (2001) evolution of deep-water sinuous channels offshore Angola (West Africa) and implications for reservoir architecture. *American Association of Petroleum Geologists Bulletin* 85, pp 1373–1405. <https://doi.org/10.1306/8626CAC3-173B-11D7-8645000102C1865D>
- CartoDEM v-3 R1 (2015) NRSC open EO data archive (NOEDA). Hyderabad: National Remote Sensing Centre. <http://bhuvan.nrsc.gov.in/data/download/index.php>
- Chen L, Khan S (2010) InSAR observation of the strike-slip faults in the northwest Himalayan frontal thrust system. *Geosphere*. 6(5):731–736. <https://doi.org/10.1130/GES00518.1>
- Clark JD, Kenyon NH, Pickering KT (1992) Quantitative analysis of the geometry of submarine channels: implications for the classification of submarine fans. *Geology*. 20(7):633–636. [https://doi.org/10.1130/0091-7613\(1992\)020<0633:QAOTGO>2.3.CO;2](https://doi.org/10.1130/0091-7613(1992)020<0633:QAOTGO>2.3.CO;2)
- Clift PD (2017) Cenozoic sedimentary records of climate-tectonic coupling in the Western Himalaya. *Prog Earth Planet Sci* 4:39–22. <https://doi.org/10.1186/s40645-017-0151-8>
- Clift PD, Henstock TJ (2015) Kongsberg EM302 processed bathymetry data, Indus Canyon and shelf, Pelagia cruise PE300 (year 2008–2009, investigators Peter Clift and Tim Henstock). Interdisciplinary Earth Data Alliance (IEDA). <http://get.iedadata.org/doi/321848>
- Clift PD, Gaedicke C, Edwards R, Lee JJ, Hildebrand P, Amjad S, White RS, Schlüter H-U (2002) The stratigraphic evolution of the Indus fan and the history of sedimentation in the Arabian Sea. *Mar Geophys Res* 23(3):223–245. <https://doi.org/10.1023/A:1023627123093>
- Clift PD, Giosan L, Henstock TJ, Tabrez AR (2014) Sediment storage and reworking on the shelf and in the canyon of the Indus River-Fan System since the last glacial maximum. *Basin Res* 26:183–202. <https://doi.org/10.1111/bre.12041>
- Corney RKT, Peakall J, Parsons DR, Elliott L, Amos KJ, Best JL, Keevil GM, Ingham DB (2006) The orientation of helical flow in curved channels. *Sedimentology* 53:249–257. <https://doi.org/10.1111/j.1365-3091.2006.00771.x>
- Damuth JE, Flood RD (1985) Amazon fan, Atlantic Ocean. In: Bouma AH, Normark WR, Barnes NE (eds) *Submarine fans and related Turbidite systems: frontiers in sedimentary geology*. Springer, New York, pp 97–106. [https://doi.org/10.1007/978-1-4612-5114-9\\_15](https://doi.org/10.1007/978-1-4612-5114-9_15)
- Darby SE, Peakall J (2012) Modelling the equilibrium bed topography of submarine meanders that exhibit reversed secondary flows. *Geomorphology* 163–164:99–109. <https://doi.org/10.1016/j.geomorph.2011.04.050>
- Deptuck ME, Sylvester Z (2018) Submarine fans and their channels, levees, and lobes. In: Micallef A, Krastel S, Savini A (eds) . *Submarine Geomorphology*, Springer Geology, pp 273–299. [https://doi.org/10.1007/978-3-319-57852-1\\_15](https://doi.org/10.1007/978-3-319-57852-1_15)
- Deptuck ME, Steffens GS, Barton M, Pirmez C (2003) Architecture and evolution of Upper Indus Fan channel-belts on the Niger Delta slope and in the Arabian Sea. *Mar Pet Geol* 20(6–8):649–676. <https://doi.org/10.1016/j.marpetgeo.2003.01.004>
- Flood RD, Damuth JE (1987) Quantitative characteristics of sinuous distributary channels on the Amazon Deep-sea Fan. *Geol Soc Am Bull* 98(6):728–738. [https://doi.org/10.1130/0016-7606\(1987\)98<728:QCOSDC>2.0.CO;2](https://doi.org/10.1130/0016-7606(1987)98<728:QCOSDC>2.0.CO;2)
- Florinsky IV (2017) An illustrated introduction to general geomorphometry. *Prog Phys Geogr* 41(6):723–752. <https://doi.org/10.1177/0309133317733667>
- Foreman BZ, Lai SYJ, Komatsu Y, Paola C (2015) Braiding of submarine channels controlled by aspect ratio similar to river. *Nat Geosci* 8: 700–703. <https://doi.org/10.1038/ngeo2505>

- Giosan L, Constantinescu S, Clift PD, Tabrez AR, Danish M, Inam A (2006) Recent morphodynamics of the Indus delta shore and shelf. *Cont Shelf Res* 26(14):1668–1684. <https://doi.org/10.1016/j.csr.2006.05.009>
- Govil P, Naidu PD (2008) Late Quaternary changes in depositional processes along the western margin of the Indus Fan. *Geo-Mar Lett* 28(1):1–6. <https://doi.org/10.1007/s00367-007-0083-1>
- Hansen L, Janocko M, Kane I, Kneller B (2017) Submarine channel evolution, terrace development, and preservation of intra-channel thin-bedded turbidites: Mahin and Avon channels, offshore Nigeria. *Mar Geol* 383(1):146–167. <https://doi.org/10.1016/j.margeo.2016.11.011>
- Imran J, Parker G, Pirmez C (1999) A nonlinear model of flow in meandering submarine and subaerial channels. *J Fluid Mech* 400:295–331. <https://doi.org/10.1017/S0022112099006515>
- Inam A, Clift PD, Giosan L, Tabrez AR, Tahir M, Rabbani MM, Danish M (2008) The geographic, geological and oceanographic setting of the Indus River. In: Gupta A (ed) *Large rivers: geomorphology and management*. Wiley, Chichester, pp 333–346. <https://doi.org/10.1002/9780470723722.ch16>
- Jarvis A, Reuter HI, Nelson A, Guevara E (2008) Hole-filled SRTM for the globe Version 4. CGIAR-CSI SRTM 90 m Database. <http://srtm.csi.cgiar.org>
- Jobe ZR, Howes NC, Auchter N (2016) Comparing submarine and fluvial channel kinematics: implications for stratigraphic architecture. *Geology* 44(11):931–934. <https://doi.org/10.1130/G38158.1>
- Kane IA, McCaffrey WD, Peakall J (2008) Controls on sinuosity evolution within submarine channels. *Geology* 36(4):287–290. <https://doi.org/10.1130/G24588A.1>
- Kazmi AH, Jan MQ (1997) *Geology and tectonics of Pakistan*. Graphic Publishers. ISBN: 9698375007, 9789698375003
- Keevil GM, Peakall J, Best JL, Amos KJ (2006) Flow structure in sinuous submarine channels: velocity and turbulence structure of an experimental submarine channel. *Mar Geol* 229(3–4):241–257. <https://doi.org/10.1016/j.margeo.2006.03.010>
- Kenyon NH, Amir A, Bishop DG, Booth DG, Campbell JM, Danish M, Davies MA, Hunter PM, Miles PR, Phipps RA, Robinson AD, Rothwell RG (1987) GLORIA study of the Indus Fan, RRS Charles Darwin Cruise 20, 31 January - 27 February 1987. Institute of Oceanographic Sciences, Deacon Laboratory, Cruise Report, No. 198, pp 17
- Kenyon NH, Amir A, Cramp A (1995) Geometry of the younger sediment bodies of the Indus Fan. In: Pickering KT, Hiscott RN, Kenyon NH, Lucchi FR, Smith RDA (eds) *Atlas of deep-water environments: architectural style in turbidite systems*. Chapman and Hall, London, pp 89–93. <https://doi.org/10.1007/978-94-011-1234-5>
- Khan IH, Clyde WC (2013) Lower Paleogene tectonostratigraphy of Balochistan: evidence for time-transgressive Late Paleocene-Early Eocene uplift. *Geosci* 3(3):466–501. <https://doi.org/10.3390/geosciences3030466>
- Khim B-K, Horikawa K, Asahara Y, Kim J-E, Ikehara M (2018) Detrital Sr-Nd isotopes, sediment provenances and depositional processes in the Laxmi Basin of the Arabian Sea during the last 800 ka. *Geol Mag* 1–13. <https://doi.org/10.1017/S0016756818000596>
- Kodagali VN, Jauhari P (1999) The meandering Indus channels: study in a small area by the multibeam swath bathymetry system-Hydrosweep. *Curr Sci* 76(2):240–243 <http://drs.nio.org/drs/handle/2264/1777>
- Kolla V (2007) A review of sinuous channel avulsion patterns in some major deep-sea fans and factors controlling them. *Mar Pet Geol* 24(6–9):450–469. <https://doi.org/10.1016/j.marpetgeo.2007.01.004>
- Kolla V, Coumes F (1987) Morphology, internal structure, seismic stratigraphy, and sedimentation of Indus Fan. *Am Assoc Pet Geol Bull* 71(6):650–677 OSTI ID: 5783289
- Kolla V, Bourges P, Urruty J-M, Safa P (2001) Evolution of deep-water sinuous channels offshore Angola (West Africa) and implications for reservoir architecture. *Am Assoc Pet Geol Bull* 85:1373–1405. <https://doi.org/10.1306/8626CAC3-173B-11D7-8645000102C1865D>
- Kolla V, Posamentier HW, Wood LJ (2007) Deep-water and fluvial sinuous channels—characteristics, similarities and dissimilarities, and modes of formation. *Mar Pet Geol* 24(6–9):388–405. <https://doi.org/10.1016/j.marpetgeo.2007.01.007>
- Konsoer K, Zinger J, Parker G (2013) Bankfull hydraulic geometry of submarine channels created by turbidity currents: relations between bankfull channel characteristics and formative flow discharge. *J Geophys Res Earth Surf* 118(1):216–228. <https://doi.org/10.1029/2012JF002422>
- Kumar A, Srivastava P (2018) Landscape of the Indus River In: *The Indian Rivers*, Singh D (ed) Springer Hydrogeology, pp 47–59. [https://doi.org/10.1007/978-981-10-2984-4\\_4](https://doi.org/10.1007/978-981-10-2984-4_4)
- Lajeunesse E, Malverti L, Lancien P, Armstrong L, Métivier F, Coleman S, ..., Parker G (2010) Fluvial and submarine morphodynamics of laminar and near-laminar flows: a synthesis. *Sedimentology* 57:1–26. <https://doi.org/10.1111/j.1365-3091.2009.01109.x>
- Leopold LB, Wolman MG (1960) River Meanders. *Geol Soc Am Bull* 71(6):769–793. [https://doi.org/10.1130/0016-7606\(1960\)71\[769:RMJ\]2.0.CO;2](https://doi.org/10.1130/0016-7606(1960)71[769:RMJ]2.0.CO;2)
- Makaske B (2001) Anastomosing rivers: a review of their classification, origin and sedimentary products. *Earth-Sci Rev* 53(3–4):149–196. [https://doi.org/10.1016/S0012-8252\(00\)00038-6](https://doi.org/10.1016/S0012-8252(00)00038-6)
- McDougall JW, Khan SH (1990) Strike-slip faulting in a foreland foldthrust belt: the Kalabagh fault and western salt range, Pakistan. *Tectonics* 9(5):1061–1075. <https://doi.org/10.1029/TC009i005p01061>
- McHargue TR, Webb JE (1986) Internal geometry, seismic facies, and petroleum potential of canyons and inner fan channels of the Indus submarine fan. *Am Assoc Pet Geol Bull* (2):70, 61–180 OSTI ID: 6968606
- McHargue TR, Pyrcz MJ, Sullivan MD, Clark JD, Fildani A, Romans BW, Covault JA, Levy M, Posamentier HW, Drinkwater NJ (2011) Architecture of turbidite channel systems on the continental slope: patterns and predictions. *Mar Pet Geol* 28(3):728–743. ISSN 0264-8172. <https://doi.org/10.1016/j.marpetgeo.2010.07.008>
- Miall AD (2002) Architecture and sequence stratigraphy of Pleistocene fluvial systems in the Malay Basin, based on seismic time-slice analysis. *Am Assoc Pet Geol Bull* 86(7):1201–1216. <https://doi.org/10.1306/61EEDC56-173E-11D7-8645000102C1865D>
- Middleton GV (1993) Sediment deposition from turbidity currents. *Annu Rev Earth Planet Sci* 21:89–114. <https://doi.org/10.1146/annurev.ea.21.050193.000513>
- Mishra R, Pandey DK, Prema R (2015) Active channel systems in the middle Indus Fan: results from high-resolution bathymetry surveys. *Curr Sci* 108(3):409–412
- Mukherjee S (2015) A review on out-of-sequence deformation in the Himalayas. In: Mukherjee S, Carosi R, van der Beek P, Mukherjee BK, Robinson DM (eds) *Tectonics of the Himalaya*. Geological Society, London, Special Publications (Vol 412). London, UK: The Geological Society. 67–109. <https://doi.org/10.1144/SP412.13>
- Murphy MA, Yin A, Kapp P, Harrison TM, Lin D, Guo J (2000) Southward propagation of the Karakoram fault system, southwest Tibet: timing and magnitude of slip. *Geology* 28(5):451–454. [https://doi.org/10.1130/0091-7613\(2000\)28<451:SPOTKF>2.0.CO;2](https://doi.org/10.1130/0091-7613(2000)28<451:SPOTKF>2.0.CO;2)
- Naini BR, Kolla V (1982) Acoustic character and thickness of sediments of the Indus Fan and the continental margin of western India. *Mar Geol* 47(3–4):181–195. [https://doi.org/10.1016/0025-3227\(82\)90068-8](https://doi.org/10.1016/0025-3227(82)90068-8)
- NCPOR (n.d.) Processed bathymetric data. Survey of the EEZ.
- Peakall J, Sumner EJ (2015) Submarine channel flow processes and deposits: a process-product perspective. *Geomorphology* 244:95–120. <https://doi.org/10.1016/j.geomorph.2015.03.005>

- Peakall J, McCaffrey B, Kneller B (2000) A process model for the evolution, morphology, and architecture of sinuous submarine channels. *J Sediment Res* 70(3):434–448. <https://doi.org/10.1306/2DC4091C-0E47-11D7-8643000102C1865D>
- Pickering KT, Clark JD, Smith RDA, Hiscott RN, Ricci Lucchi F, Kenyon N (1995) Architectural element analysis of turbidite systems, and selected topical problems for sand-prone deep-water systems. In: Pickering KT, Hiscott RN, Kenyon NH, Lucchi FR, Smith RDA (eds) *Atlas of deep-water environments: architectural style in turbidite systems*. Chapman and Hall, London, pp 1–11. [https://doi.org/10.1007/978-94-011-1234-5\\_1](https://doi.org/10.1007/978-94-011-1234-5_1)
- Pike RJ (1995) Geomorphometry-diversity in quantitative surface analysis. *Prog Phys Geogr* 24(1):1–20. <https://doi.org/10.1177/030913330002400101>
- Pike RJ, Evans IS, Hengl T (2009) Geomorphometry: a brief guide. In: Hengl T, Reuter H-I (eds) *Developments in Soil Science*, volume 33. Elsevier, pp 3–30
- Pirmez C, Flood RD (1995) Morphology and structure of Amazon Channel. *Proceedings of the Ocean Drilling Program, Initial Report*, 155, Chapter 3, pp 23–45. <https://doi.org/10.2973/odp.proc.ir.155.103.1995>
- Posamentier HW (2003) Depositional elements associated with a basin floor channel-levee system: case study from the Gulf of Mexico. *Mar Pet Geol* 20(6–8):677–690. <https://doi.org/10.1016/j.marpetgeo.2003.01.002>
- Prema R, Pandey DK, Mahender K (2018) Longitudinal profiling and elevation-relief analysis of the Indus. *Arab J Geosci* 11:343–318. <https://doi.org/10.1007/s12517-018-3657-5>
- Prins MA, Postma G, Cleveringa J, Cramp A, Kenyon NH (2000) Controls on terrigenous sediment supply to the Arabian Sea during the late Quaternary: the Indus Fan. *Mar Geol* 169(3–4):327–349. [https://doi.org/10.1016/S0025-3227\(00\)00086-4](https://doi.org/10.1016/S0025-3227(00)00086-4)
- Qin Y, Alves TM, Constantine J, Gamboa D (2016) Quantitative seismic geomorphology of a submarine channel system in SE Brazil (Espírito Santo Basin): scale comparison with other submarine channel systems. *Mar Pet Geol* 78:455–473. <https://doi.org/10.1016/j.marpetgeo.2016.09.024>
- Schumm SA, Khan HR (1972) Experimental study of channel patterns. *Geol Soc Am Bull* 83(6):1755–1770. [https://doi.org/10.1130/0016-7606\(1972\)83\[1755:ESOC\]2.0.CO;2](https://doi.org/10.1130/0016-7606(1972)83[1755:ESOC]2.0.CO;2)
- Searle MP (1996) Geological evidence against large-scale pre-Holocene offsets along the Karakoram fault: implications for the limited extrusion of the Tibetan plateau. *Tectonics* 15(1):171–186. <https://doi.org/10.1029/95TC01693>
- Shanmugam G, Muiola RJ (1988) Submarine fans: characteristics, models, classification, and reservoir potential. *Earth Sci Rev* 24(6):383–428. [https://doi.org/10.1016/0012-8252\(88\)90064-5](https://doi.org/10.1016/0012-8252(88)90064-5)
- Shareef NM, Dinesh AC, Venkateswara R, Jayaprakash C, Rajarama KN, Varghese S, Girishbai D (2018) Evidences of shallow marine sediments as channel fill in the lower Indus Fan. *Indian J Geo-Marine Sci* 47:67–72 <http://nopr.niscair.res.in/handle/123456789/43453>
- Smith WHF, Sandwell DT (1997) Global seafloor topography from satellite altimetry and ship depth soundings. *Science* 277(5334):1957–1962. <https://doi.org/10.1126/science.277.5334.1956>
- Stow DAV, Howell DG, Nelson CH (1985) Sedimentary, tectonic, and sea-level controls. In: Bouma AH, Normark WR, Barnes NE (eds) *Submarine fans and related turbidite systems*. (1st ed.). *Frontiers in Sedimentary Geology*. Springer, New York. [https://doi.org/10.1007/978-1-4612-5114-9\\_4](https://doi.org/10.1007/978-1-4612-5114-9_4)
- von Rad U, Tahir M (1997) Late Quaternary sedimentation on the outer Indus shelf and slope (Pakistan): evidence from high-resolution seismic data and coring. *Mar Geol* 138(3–4):193–236. [https://doi.org/10.1016/S0025-3227\(96\)00090-4](https://doi.org/10.1016/S0025-3227(96)00090-4)
- Ward B (2007) Anammox and denitrification in the ODZ of the Arabian Sea. Cruise: KNOX09RR, Kongsberg EM120 multibeam sonar data. Princeton University. R/v Roger Revelle, Scripps Institution of Oceanography. Marine Geophysical Data System. <https://doi.org/10.7284/903735>
- Whitmarsh RB, Weser OE, Ali S, Boudreaux JE, Fleisher RL, Jipa D, ..., Hamilton N (1974) Site 220, initial reports of the deep sea drilling project.23, pp 117–166. Publisher: Texas A&M University, Ocean Drilling Program, College Station, TX, United States. ISSN: 0080-8334. <https://doi.org/10.2973/dsdp.proc.23.104.1974>
- Winston Y, Yang Y-C, Savitsky A, Alford D, Brown C, Wescoat J, Debowicz D, Robinson S (eds) (2013) *Hydrology and glaciers in the upper Indus Basin*. In: *the Indus Basin of Pakistan: the impacts of climate risks on water and agriculture*. The World Bank, Washington DC, pp 57–75. <https://doi.org/10.1596/978-0-8213-9874-6>
- Wynn RB, Cronin BT, Peakall J (2007) Sinuous deep-water channels: genesis, geometry and architecture. *Mar Pet Geol* 24(6–9):341–387. <https://doi.org/10.1016/j.marpetgeo.2007.06.001>
- Yin AN (2006) Cenozoic tectonic evolution of the Himalayan orogen as constrained by along-strike variation of structural geometry, exhumation history, and foreland sedimentation. *Earth Sci Rev* 76:1–131. <https://doi.org/10.1016/j.earscirev.2005.05.004>

**Publisher's note** Springer Nature remains neutral with regard to jurisdictional claims in published maps and institutional affiliations.